SUPPORTING INFORMATION

Bio-Inspired Mn(I) Complexes for the Hydrogenation of CO_2 to Formate and Formamide

Abhishek Dubey[†], Luca Nencini[‡], Robert R. Fayzullin[§], Carlo Nervi*[,‡], and Julia R. Khusnutdinova*[,†]

[†]Coordination Chemistry and Catalysis Unit, Okinawa Institute of Science and Technology, 1919-1 Tancha, Onna-son, Okinawa, Japan

[‡]Department of Chemistry, University of Turin, Via P. Giuria 7, 10125, Turin, Italy

[§]A. E. Arbuzov Institute of Organic and Physical Chemistry, Kazan Scientific Center, Russian Academy of Sciences, Arbuzov Street 8, Kazan 420088, Russian Federation

Email: juliak@oist.jp and carlo.nervi@unito.it

Table of contents

General specifications

All manipulations were carried out under a nitrogen atmosphere using standard Schlenk and glove box techniques if not indicated otherwise. All reagents for which synthesis is not given were commercially available from Sigma-Aldrich, TCI, Nacalai Tesque and were used as received without further purification. Solvents were purified prior to use by passing through a column of activated alumina using an MBRAUN SPS. Complexes **2**,[1] **5**[2] and ligands 6,6'-dimethoxy-2,2'-bipyridine[3] and 4,4'-dihydroxy-2,2'-bipyridine[4] were prepared according to the literature procedures and their spectroscopic characteristics matched those reported in the literature. NMR spectra were recorded on JEOL ECZ600R 600MHz, JEOL ECZ400S 400 MHz or Bruker Avance II 400 MHz spectrometers. Chemical shifts are reported in ppm and referenced to residual solvent resonance peaks. Abbreviations for the multiplicity of NMR signals are s (singlet), d (doublet), t (triplet), q (quartet), m (multiplet), br (broad), vt (virtual triplet). UV-visible spectra were recorded on an Agilent Cary 60 spectrophotometer. A Thermo Scientific Hybrid Mass Spectrometer (LTQ Orbitrap) was used for high resolution mass spectrometry (HRMS) data collection. The mass spectrometer was equipped with a high-pressure liquid chromatography instrument (HPLC) (Paradigm MS4, Michrom Bioresources Inc.), an autosampler (HTC PAL, CTC Analytics) and a nanoelectrospray ion source (NSI). IR spectra were recorded using an Agilent Cary 630 spectrometer with a diamond ATR module. IR spectroscopy abbreviations are as follows: w (weak), m (medium), s (strong); br (broad), sh (shoulder). Elemental analyses were performed using an Exeter Analytical CE440 instrument or carried out by A Rabbit Science (Sagamihara City, Kanagawa prefecture). GC-MS analysis was performed using a Shimadzu GCMS-QP2010 equipped with a Shimadzu SH-Rxi-1ms 30 meter column.

Hydrogenation experiments were performed using a Taiatsu Techno custom-designed high pressure multireactor in 50 mL stainless steel autoclaves equipped with Teflon inserts and magnetic stirring bars. The temperature was controlled by using an internal thermocouple and was stable within a range of 1 ^{o}C.

Preparation of ligands and Mn complexes.

General note: All syntheses were carried out under an atmosphere of N_2. Reaction were covered with aluminium foil (to avoid exposure to light) and all synthesized compounds were stored in the dark at 0 ^{o}C.

Preparation of [Mn(6,6'-dihydroxy-2,2'-bipyridine)(CO)$_3$Br], 1

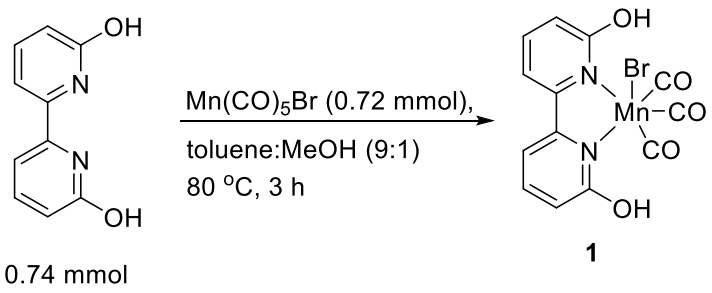

A suspension of 6,6'-dihydroxy-2,2'-bipyridine (140 mg, 0.74 mmol) and $Mn(CO)_5Br$ (200 mg, 0.72 mmol) in toluene:MeOH (9:1, 30 mL) was heated for 3 hours at 80 ^{o}C, and then placed in the refrigerator (0 ^{o}C) overnight. Hexane was added to the cold solution, and the resulting orange precipitate was filtered off and washed with diethyl ether. The final product was recrystallized from acetone and diethyl ether, and dried in vacuum for 24 hours. Isolated as a yellowish orange solid. 0.242 g (0.596 mmol), yield 82%

^{1}H NMR (400 MHz, acetone-d_6, 23 ^{o}C), δ: 3.76 (br s, 2H, OH), 7.06-7.08 (m, 2H, Py), 7.88-7.94 (m, 4H, Py).

^{13}C NMR (101 MHz, DMF-d_7, 23 ^{o}C), δ_c: 110.8, 114.4, 140.6, 156.1, 165.9, 205.9.

FT-IR (solid): 3076 (br, m), 2018 (s, CO), 1902 (br, s, CO), 1602 (m), 1580 (w), 1479 (m), 1431 (m), 791 (m) cm^{-1}.

ESI-HRMS (*m/z pos*): calculated for [$C_{13}H_8MnN_2O_5$]: 326.9808; found: 326.9810 [M-Br]$^{+}$

Anal. Calcd for **1**, $C_{13}H_8BrMnN_2O_5$: C, 38.36; H, 1.98; N, 6.88. Found: C, 38.10; H, 1.99; N, 6.82.

X-ray quality crystals were obtained by diethyl ether vapor diffusion into acetone solution.

Preparation of [Mn(6,6'-dimethoxy-2,2'-bipyridine)(CO)$_3$Br], 3

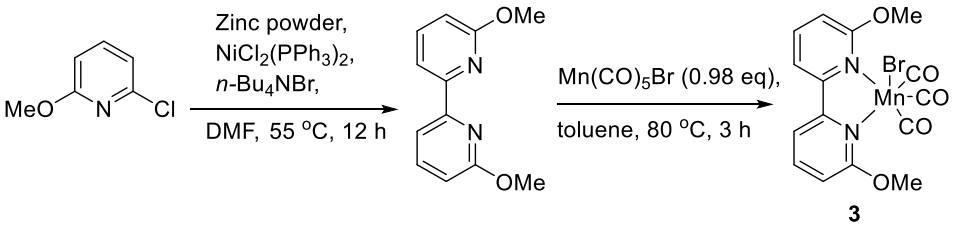

6,6'-Dimethoxy-2,2'-bipyridine was prepared following the literature procedure.[3] In a three-necked 100 mL round bottom flask, 1.37 g (2.1 mmol) of bis(triphenylphosphine)nickel(II)dichloride, 452 mg (6.95 mmol) of zinc, and 2.23 g (6.95 mmol) tetrabutylammonium bromide were dissolved in 40 mL of DMF. After degassing, the solution was stirred at room temperature for 30 min (the green starting solution turns brown after this time). To this solution, 1 g (6.96 mmol) of 3-chloro-6-methoxypyridine is added and the reaction mixture was heated at 55 °C for 12 hours. After evaporation of the solvent under reduced pressure, the residue was taken up in a saturated solution of ammonium chloride, the suspension was extracted with 4 x 40 ml of dichloromethane and the organic phase was dried over $MgSO_4$, filtered, and then concentrated under reduced pressure. The crude mixture obtained was chromatographed on silica gel (eluent: ethyl acetate : hexane = 2:98) to yield the 6,6'-dimethoxy-2,2'-bipyridine. White crystalline solid, 0.665 g (3.07 mmol), yield 88%

^{1}H NMR (400 MHz, $CDCl_3$, 23 °C), δ: 4.03 (s, 6H, OMe), 6.74 (d, J = 8.2 Hz, 2H, Py), 7.68 (vt, J ~ 7.8 Hz, 2H, Py), 8.01 (d, J = 7.4 Hz, 2H).

^{13}C NMR (101 MHz, $CDCl_3$), δ_c: 53.2, 110.9, 113.6, 139.2, 153.3, 163.4.

ESI-HRMS (*m/z pos*): calculated for $[C_{15}H_{12}MnN_2O_5]$: 217.0972; found: 217.0970

[Mn(6,6'-dimethoxy-2,2'-bipyridine)(CO)$_3$Br] (**3**): A suspension of 6,6'-dimethoxy-2,2'-bipyridine (160 mg, 0.74 mmol) and $Mn(CO)_5Br$ (200 mg, 0.72 mmol) in toluene (20 mL) was heated for 3 hours at 80 °C. The solvent was removed by vacuo and the resulting orange-red solid was washed with cold diethyl ether, and dried under vacuum. The final product was recrystallized from acetone and diethyl ether and then dried in vacuum for 24 hours. Isolated as a yellowish orange solid, 0.247 g (0.567 mmol), yield 78%.

^{1}H NMR (400 MHz, CD_3CN), δ: 4.16 (s, 6H, OMe), 7.14 (d, J = 8.1 Hz, 2H), 7.93 (d, J = 7.8 Hz, 2H), 8.05 (vt, J ~8.0 Hz, 2H, Py).

^{13}C NMR (101 MHz, DMF-d_7, 23 °C), δ_c: 56.8, 107.9, 116.5, 142.1, 156.3, 166.3 (CO peak is not clearly seen likely due to broadening or low intensity).

FT-IR: 3088 (w), 2009 (s, CO), 1892 (br, CO), 1600 (w), 1566 (w), 1478 (m), 1419 (w), 1293 (w), 1270 (m), 1024 (m), 790 (m) cm^{-1}.

ESI-HRMS (*m/z pos*): calculated for $[C_{15}H_{12}MnN_2O_5]$: 355.0121; found: 355.0118$[M\text{-}Br]^+$

Anal. Calcd for **3**, $C_{15}H_{12}BrMnN_2O_5$: C, 41.41; H, 2.78; N, 6.44. Found: C, 41.31; H, 2.54; N, 6.38.

X-ray quality crystals were obtained by diethyl ether vapor diffusion into acetone solution.

Preparation of [Mn(6,6'-diamino-2,2'-bipyridine)(CO)$_3$Br], 4

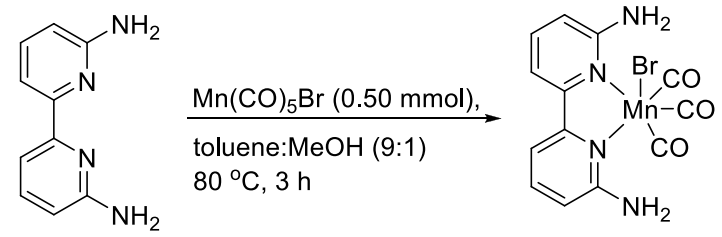

0.51 mmol **4**

A solution of 6,6'-diamine-2,2'-bipyridine (95 mg, 0.51 mmol) in 1 mL of methanol was added to a solution of $Mn(CO)_5Br$ (137 mg, 0.50 mmol) in toluene (9 mL). The mixture was heated for 3 hours at 80 °C, and then placed in the refrigerator (0 °C) overnight. Hexane was added to the cold solution, and the resulting orange precipitate was filtered off and washed with diethyl ether. The final product was recrystallized from acetone and diethyl ether, and dried in vacuum for 24 hours. Isolated as an orange solid, 0.171 g (0.423 mmol), yield 85%.

^{1}H NMR (400 MHz, acetone-d_6, 23 °C), δ: 3.74 (br s, 2H, NH), 6.61 (br d, J = 12.8 Hz, 2H, NH), 6.93 (d, J = 8.1 Hz, 2H, Py), 7.61 (d, J = 7.6 Hz, 2H, Py), 7.72 (vt, J ~ 7.7 Hz, 2H, Py).

^{13}C NMR (101 MHz, acetone-d_6, 23 °C), δ_c: 111.2, 111.7, 139.2, 154.2, 162.8, 209.4.

FT-IR (solid): 3412 (w), 3323 (m), 2022 (m), 1944 (m), 1920 (sh, s), 1904 (s, CO), 1615 (m), 1597 (w), 1477 (m) and 782 (m) cm^{-1}.

ESI-HRMS (*m/z pos*): calculated for $[C_{13}H_8MnN_2O_5]$: 326.9808; found: 326.9810 $[M\text{-}Br]^+$

Anal. Calcd for **4**, $C_{13}H_{10}BrMnN_4O_3$: C, 38.55; H, 2.49; N, 13.83. Found: C, 38.35; H, 2.45; N, 13.87.

X-ray quality crystals were obtained by diethyl ether vapor diffusion into acetone solution.

Preparation of [Mn(6,6'-dihydroxy-2,2'-bipyridine)(CO)$_3$(MeCN)] (OTf), 6

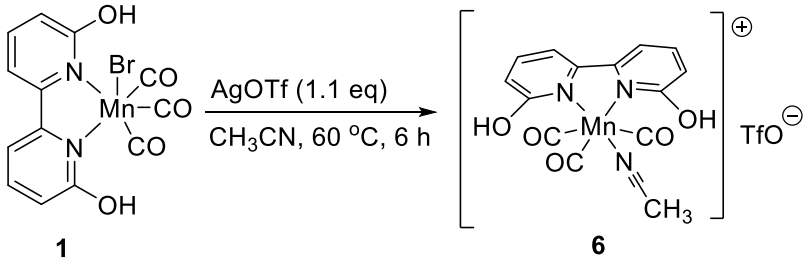

1 **6**

Complex **1** (203 mg, 0.5 mmol) was mixed with silver trifluoromethanesulfonate (AgOTf, 141 mg, 0.55 mmol) in a 50 mL Schlenk flask with 20 mL acetonitrile (MeCN) in the glovebox. The reaction flask was brought out of the box, covered with foil (to avoid exposure to light), and heated at 60 °C for 6 hours. The resulting precipitated AgBr was removed by filtration. The solvent was removed by vacuum and the resulting solid was washed with ether. The final

product was recrystallized from acetonitrile and diethyl ether, and dried in vacuum for 24 hours. Isolated as a yellow solid 0.193 g (0.374 mol), yield 75%.

^{1}H NMR (400 MHz, CD_3CN, 23 °C), δ: 7.11 (d, J = 8.2 Hz, 2H, Py), 7.83 (d, J = 7.7 Hz, 2H, Py), 7.95 (vt, J ~ 8.0 Hz, 2H, Py), 10.10 (s, 2H, OH).

^{13}C NMR (151 MHz, CD_3CN, -30 °C), δ_c: 112.2, 115.4, 126.7, 141.9, 154.9, 165.6, 218.7, 220.1.

FT-IR (solid): 3146 (br, OH), 2041 (m, CN), 1961 (m, CO), 1923 (br, s, CO), 1605 (w), 1587 (w), 1482 (m), 1435 (m), 1282 (m), 1211 (s, OTf), 1163 (s, OTf), 1025 (s, OTf), 975 (m), 800 (m) cm^{-1}.

ESI-HRMS (*m/z pos*): calculated for $[C_{15}H_{11}MnN_3O_5]$: 368.0074; found: 368.0075$[M\text{-}OTf]^+$

Anal. Calcd for **6**, $C_{16}H_{11}F_3MnN_3O_8S$: C, 37.15; H, 2.14; N, 8.12. Found: C, 37.19; H, 2.13; N, 7.94.

X-ray quality crystals were obtained by diethyl ether vapor diffusion into acetonitrile solution.

Preparation of [Mn(6,6'-dimethoxy-2,2'-bipyridine)(CO)$_3$(MeCN)](OTf), 7

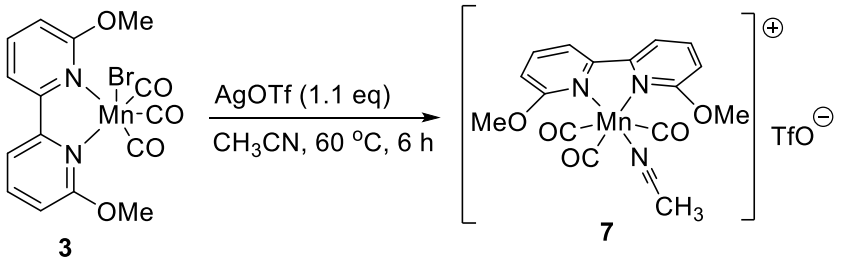

3 **7**

Complex **3** (131 mg, 0.3 mmol) was mixed with silver trifluoromethanesulfonate (AgOTf, 85 mg, 0.33 mmol) in a 50 mL Schlenk flask with 10 mL acetonitrile (MeCN) in the glovebox. The reaction flask was brought out of the box, covered with foil (to avoid exposure to light), and heated at 60 °C for 6 hours. The resulting precipitated AgBr was removed by filtration. The solvent was removed by vacuum and the resulting solid was washed with ether. The final product was recrystallized from acetonitrile and diethyl ether, and dried in vacuum for 24 hours. Isolated as a yellow solid, 0.130 g (0.237 mmol), yield 79%.

^{1}H NMR (400 MHz, CD_3CN, 23 °C), δ: 4.16 (s, 6H, OMe), 7.23 (d, J = 8.4 Hz, 2H, Py), 7.97 (d, J = 7.8 Hz, 2H, Py), 8.14 (vt, J~8.0 Hz, 2H, Py).

^{13}C NMR (101 MHz, CD_3CN, 23 °C), δ_c: 56.8, 108.9, 116.5, 126.7, 142.8, 155.3, 166.6 (CO signal could not be seen likely due to broadening or low intensity).

FT-IR (solid): 310 (w), 2982 (w), 2862 (w), 2037 (s, CN), 1940 (s, CO), 1921 (br, s, CO), 1602 (w), 154 (w), 1482 (m), 1424 (w), 1252 (s), 1224 (s), 1145 (s, OTf), 1029 (s, OTf), 792 cm^{-1}.

ESI-HRMS (*m/z pos*): calculated for $[C_{17}H_{15}MnN_3O_5]$: 396.0387; found: 396.0391$[M\text{-}OTf]^+$

Anal. Calcd for **7**, $C_{18}H_{15}F_3MnN_3O_8S$: C, 39.65; H, 2.54; N, 7.71. Found: C, 39.57; H, 2.64; N, 7.53.

X-ray quality crystals were obtained by diethyl ether vapor diffusion into acetonitrile solution.

Preparation of [Mn(4,4'-dihydroxy-2,2'-bipyridine)(CO)$_3$(MeCN)](OTf), 8

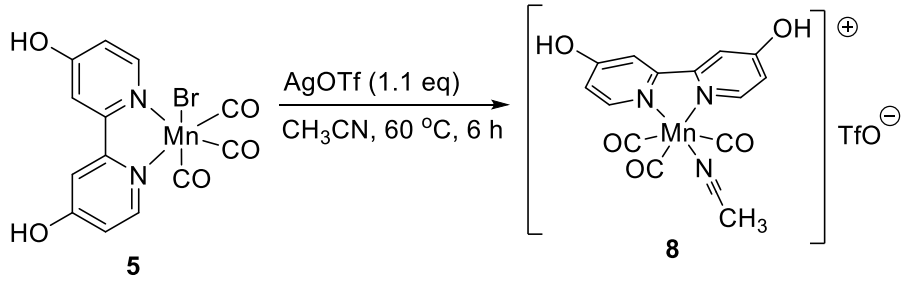

5 **8**

Complex **5** (122 mg, 0.3 mmol) was mixed with silver trifluoromethanesulfonate (AgOTf, 85 mg, 0.33 mmol) in a 50 mL Schlenk flask with 10 mL acetonitrile (MeCN) in the glovebox. The reaction flask was brought out of the box, covered with foil (to avoid exposure to light), and heated at 60 °C for 6 hours. The resulting precipitated AgBr was removed by filtration. The solvent was removed by vacuum and the resulting solid was washed with ether. The final product was recrystallized from acetonitrile and diethyl ether, and dried in vacuum for 24 h. Isolated as a yellow solid, 0.107 g (0.206 mmol), 69% yield.

^{1}H NMR (600 MHz, CD_3CN, -30 °C), δ: 7.08 (slightly broadened d, J ~ 5.1 Hz, 2H, Py), 7.71 (s, 2H, Py), 8.7 (d, J = 5.5 Hz, 2H, Py), 9.27 (br s, 2H, OH).

^{13}C NMR (151 MHz, CD_3CN, -30 °C), δ_c: 111.1, 114.8, 126.6, 154.9, 157.4, 166.8, 218.6 (carbonyl peaks could not be detected due to broadening of the peaks and low intensity).

FT-IR (solid): 3185, 2038 (s, CN), 1948 (sh, s, CO), 1929 (br, s, CO), 1622 (w), 1578 (w), 1473 (w), 1283 (m) 1216 (s, OTf), 1168 (s, OTf) and 1028 (s, OTf), 837 (m) cm^{-1}.

ESI-HRMS (*m/z pos*): calculated for [$C_{15}H_{11}MnN_3O_5$]: 368.0074; found: 368.0073 [M-OTf]$^+$

Anal. Calcd for **8**, $C_{16}H_{11}F_3MnN_3O_8S$: C, 37.15; H, 2.14; N, 8.12. Found: C, 37.05; H, 2.11; N, 8.06.

Catalytic hydrogenation procedures

Representative experiment for CO_2 hydrogenation to formate in the presence of a base:

A fresh stock solution of complex **1** (8.14 mg in 8.0 mL 1,4-dioxane or acetonitrile) was prepared prior to the experiment. Under a nitrogen atmosphere, 2.0 mL of a stock solution of complex **1** (containing 5 μmol of **1**), DBU (6.5 mmol) and 1,4-dioxane or acetonitrile were mixed in a vial (total volume of 5.0 mL) and stirred briefly. The yellow, clear solution was transferred into a 50 mL stainless steel autoclave equipped with a Teflon insert and a Teflon-coated magnetic stirring bar. All gas connections were purged 5 times with nitrogen (0.6 MPa), then the autoclave was subsequently pressurized with CO_2 (3 MPa) and hydrogen (additional 3 MPa to total pressure of 6 MPa). The reaction mixture was magnetically stirred at 400 rpm and heated using a heating mantle. The temperature inside the reaction was measured and controlled using an internal thermocouple inserted into the stainless steel sheath immersed in the solution. After 24 hours of heating at the desired temperature, the autoclave was cooled down to RT and depressurized. Internal standard (DMF) was added to the reaction mixture using a microsyringe. A sample of the reaction mixture was dissolved in D_2O and analyzed by ^1H NMR using a relaxation delay time of 10 s. Yields were determined vs. DMF as an internal standard. DMF was stable under the conditions of reaction mixture analysis (r.t. 1atm air). Control experiments showed that what no formate was formed in the absence of Mn catalyst or in the presence of $Mn(CO)_5Br$.

Additional data showing optimization of the reaction conditions, use of various solvents, bases and control experiments, are given in Tables S1-S3.

Representative NMR spectra are shown in Figures S23-S36.

Representative experiment for formamide formation:

Under a nitrogen atmosphere, 2.0 mL of stock solution of complex **1** prepared as above (containing 5 μmol of **1**), diethylamine (2 mmol) and 1,4-dioxane were mixed in a vial (total volume of 5.0 mL) and stirred briefly. The yellow, clear solution was transferred into a 50 mL stainless steel autoclave equipped with a Teflon insert and a Teflon-coated magnetic stirring bar. All gas connections were purged 5 times with nitrogen (0.6 MPa), then the autoclave was pressurized with CO_2 and then with hydrogen. The reaction mixture was magnetically stirred at 400 rpm and heated using a heating mantle. The temperature inside the reaction was measured and controlled using an internal thermocouple inserted into the stainless steel sheath immersed in the solution. After 24 hours of heating at the desired temperature, the autoclave was cooled down to RT and depressurized. Internal standard, pre-weighed 1,3,5-trimethoxybenzene, was added to the reaction mixture. A sample of the reaction mixture was dissolved in $CDCl_3$ and analyzed by ^1H NMR using a relaxation delay time of 10 s. Yields were determined by NMR vs. 1,3,5-trimethoxybenzene as the internal standard. The

formation of formamide product was confirmed by NMR by comparison with literature data. The reaction mixtures were also analyzed by GC-MS to further identify the formamide products. Trace amounts of formate salt were also observed. Control experiments have shown what no formamide was formed in the absence of Mn catalyst or in the presence of complex **2**. Additional data showing optimization of the reaction conditions and control experiments are given in Tables S5-S7.

Representative NMR spectrum is shown in Figure S37.

Additional tables for Mn-catalyzed CO_2 hydrogenation

Table S1. Hydrogenation of CO_2 in the presence of various bases catalyzed by complexes **1** or **6**.[a]

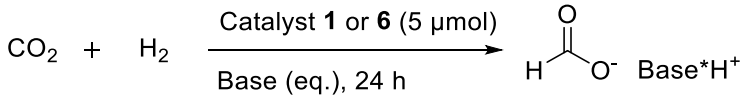

entry	complex	base (equiv)[b]	T, °C	solvent	TON[c]
1	**1**	2M KOH	80	H_2O	N.D.[d]
2	**1**	Et_3N (1000)	80	Dioxane	19
3	**6**	KO^{t}Bu(100)	80	Dioxane	11
4	**6**	Pyridine (1000)	80	Dioxane	N.D.
5	**6**	NaOMe (100)	80	Dioxane	N.D.
6	**6**	Cs_2CO_3 (100)	80	Dioxane	N.D.
7	**6**	DABCO[e] (1000)	80	Dioxane	194
8	**6**	Et_3N (1000)	80	Dioxane	N.D.
9[f]	**6**	Et_3N (10000)	65	Et_3N	244
10	**6**	Et_3N (1000)	65	MeCN	282

[a] Typical conditions: **1** or **6** (5 μmol), base, solvent (5 mL), H_2 (3 MPa), CO_2 (3 MPa), 65 °C or 80 °C, 24 h. [b] Amount of base is indicated in parentheses as number of equivalents relative to Mn complex. [c] TON = mmol formate/mmol catalyst; amount of formate was determined by NMR integration relative to DMF standard added to reaction mixture after completion. [d] N.D. = not detected. [e] DABCO = 1,4-diazabicyclo[2.2.2]octane. [f] Et_3N is used in the amount of 50 mmol serving both as a base and as a solvent.

Table S2. Hydrogenation of CO_2 to formate in various solvents.[a]

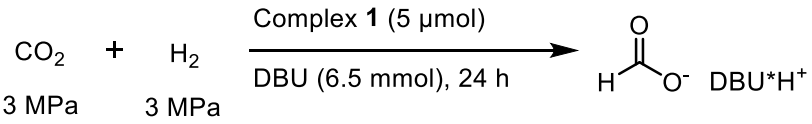

entry	solvent	T, °C	TON[b]
1	THF	65	924
2	EtOH	80	334
3	MeOH	65	-
4[d]	Dioxane-H_2O	80	302
5[d]	MeCN-H_2O	65	428
6[d]	THF-H_2O	65	244
7[d]	EtOH-H_2O	80	240

[a] Typical conditions: **1** (5 μmol), base (6.5 mmol), solvent (5 mL), H_2 (3 MPa), CO_2 (3 MPa), 65 °C or 80 °C, 24 h. [b] TON = mmol formate/mmol catalyst; amount of formate was determined by NMR integration relative to DMF standard added to reaction mixture after completion. [c] yield = (mmol formate*100%)/mmol DBU (based on DBU:formate 1:1); determined by integration of formate peak relative to DBU. [d] H_2O was used in the amount of 1000 equivalents relative to Mn complex.

Table S3. Control experiments for hydrogenation of CO_2 to formate.[a]

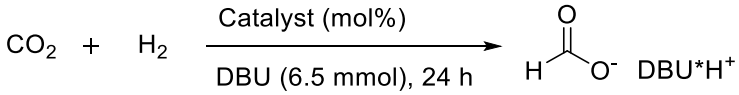

In all cases, no formate was detected in the reaction mixtures.

entry	Catalyst (mol%)	base	T, °C	solvent	TON[b]
1	$Mn(CO)_5Br$ (1 mol%)	DBU	65	MeCN	N.D.[c]
2	$Mn(CO)_5Br$ (1 mol%)	DBU	80	Dioxane	N.D.
3	Complex **1** (0.5 mol%)	**None**	65	MeCN	N.D.
4	6,6'-dihydroxy-2,2'-bipyridine (1 mol%)	DBU	65	MeCN	N.D.
5	None	DBU	65	Dioxane	N.D.

[a] Typical conditions: Solvent (5 mL), H_2 (3 MPa), CO_2 (3 MPa), 65 °C or 80 °C, 24 h. [b] TON = mmol formate/mmol catalyst; amount of formate was determined by NMR integration relative to DMF standard added to reaction mixture after completion. [c] N.D. = not detected.

Mercury Test

Mercury poisoning test was performed as follows to estimate possible presence of heterogeneous catalysts that would be inhibited in the presence of metallic mercury. Under same reaction conditions as used in Table 1, entry 2, the reaction was performed in the presence of a drop of metallic mercury. The TON of 1160 was observed (average of two runs), corresponding to 95% yield of DBU. This suggests that no inhibition is observed.

Table S4. Comparison at short reaction times and estimation of TOF.[a]

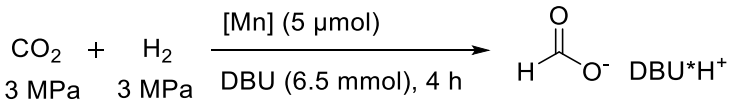

entry	solvent	complex	T, °C	TON[b]	TOF [h^{-1}][c]
1	Dioxane	**1**	80	640	160
2	MeCN	**1**	65	954	238
3	MeCN	**2**	65	10	2.5
4	MeCN	**3**	65	6	1.5
5	MeCN	**4**	65	22	5.5
6	MeCN	**5**	65	72	18
7	MeCN	**6**	65	596	149
8	MeCN	**7**	65	32	8
9	MeCN	**8**	65	100	20

[a] Typical conditions: [Mn] (5 μmol), base (6.5 mmol), solvent (5 mL), H_2 (3 MPa), CO_2 (3 MPa), 65 °C or 80 °C, 4 h. [b] TON = mmol formate/mmol catalyst; amount of formate was determined by NMR integration relative to DMF standard added to reaction mixture after completion; average of two runs. [c] TOF is estimated as TON/hours over 4 h reaction time only for qualitative comparison of various catalysts at shorter reaction times.

Table S5. Optimization of H_2 and CO_2 pressure for hydrogenation of CO_2 to formamide in the presence of diethylamine.[a]

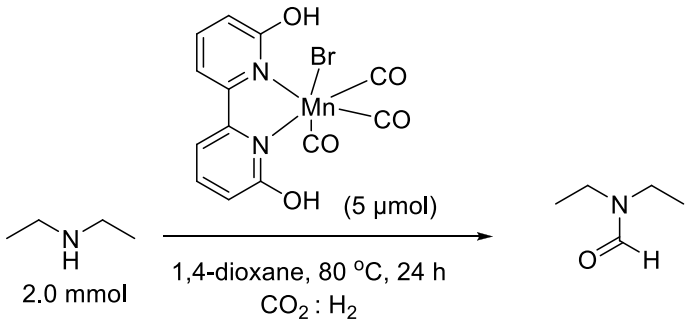

entry	pCO_2, MPa	pH_2, MPa	TON[b]
1	1	1	78
2	1	3	170
3	2	2	105
4	2	4	205
5	2	5	248
7	3	5	210

[a] Typical conditions: **1** (5 μmol), Et_2NH (2.0 mmol), solvent (5 mL), H_2, CO_2, 80 °C, 24 h. [b] TON = mmol formamide/mmol catalyst; amount of formamide was determined by NMR integration relative to DMF standard added to reaction mixture after completion.

Table S6. Effect of temperature on formamide formation.[a]

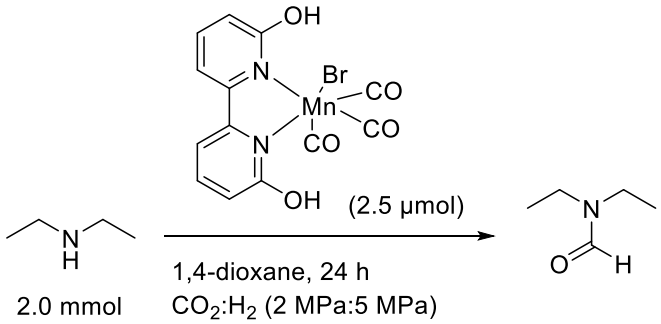

entry	T, °C	TON[b]	yield, %[c]
1	60	96	12
2	80	581	68
3	100	387	48
4	120	179	21

[a] Typical conditions: **1** (5 μmol), Et_2NH (2.0 mmol), solvent (5 mL), H_2 (5 MPa) CO_2 (2 MPa), 24 h. [b]TON = mmol formamide/mmol catalyst; amount of formamide was determined by NMR integration relative to DMF standard added to reaction mixture after completion. [c] yield determined by NMR integration of formamide *H*CO peak against DMF standard.

Table S7. Control experiments for formamide formation.[a]

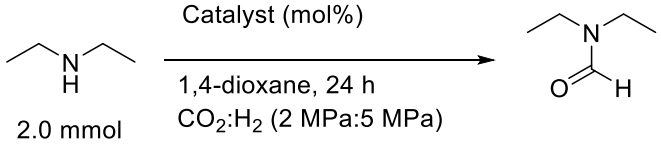

entry	Catalyst (mol%)	Formamide yield, %[b]
1	$Mn(CO)_5Br$ (1 mol%)	trace
2	None	N.D.
3	Complex **2** (1 mol%)	N.D.

[a] Typical conditions: Et_2NH (2.0 mmol), solvent (5 mL), H_2 (5 MPa) CO_2 (2 MPa), 24 h. [b] yield determined by NMR integration of formamide *H*CO peak against DMF standard. N.D. = not detected.

Reactivity of complex 6 with DBU in the presence of H_2, CO_2 or H_2-CO_2 mixtures followed by NMR.

Reactivity of complex 6 with DBU

A Wilmad pressure NMR tube (medium wall thickness) was charged with 5.6 mg of complex **6** in 0.5 mL of CD_3CN. The first NMR spectrum was recorded at RT and showed pyridyl multiplets at 7.11, 7.83, and 7.97 ppm (Figure S17). Then 3.0 equiv of DBU were added. The NMR spectrum was recorded again at RT showing that the pyridyl multiplets shifted to 6.08, 6.72 and 7.18 ppm. (Figure S1). The room temperature spectrum shows multiplet broadening. Upon cooling the CD_3CN solution to -30 °C, broadening decreases, but cannot be completely resolved.

^{1}H NMR of **6** after addition of 3 equiv of DBU: (600 MHz, CD_3CN, -30 °C): 6.08 (br d, J ~ 7.5 Hz, 2H), 6.72 (br d, J ~ 5.7 Hz, 2H), 7.18 (br d, J ~ 6 Hz, 2H), 12.28 (br s, 2H).

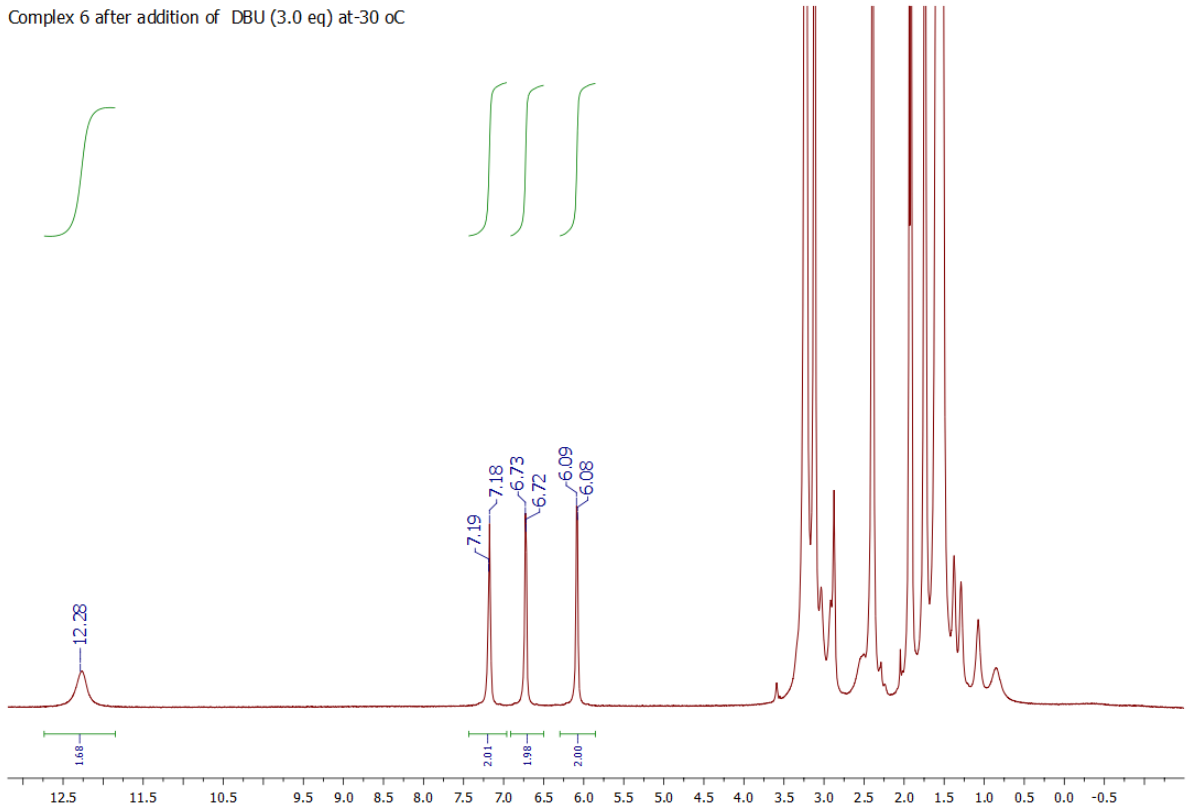

Figure S1. ^{1}H NMR spectrum of complex **6** after reaction with DBU in CD_3CN (-30 °C).

We also studied reactivity of complex **8** with DBU. A NMR spectrum was recorded at -30 °C showing pyridyl multiplets shifted by ca. 1 ppm (Py multiplets at 6.19, 6.75, and 8.06 ppm) and appearance of a broad singlet at 11.40 ppm.

Reactivity of complex 6 in the presence of DBU and H_2

A Wilmad pressure NMR tube (medium wall thickness) was charged with 5.6 mg of complex **6** in 0.5 mL of CD_3CN. Then 3.0 equiv of DBU were added. The NMR tube was pressurized to 5 bar pressure using H_2. An NMR spectrum was recorded at -30 °C. (Figure S2) showing pyridyl multiplets at 6.09, 6.73 and 7.18 ppm (analogous to those observed in the absence of H_2, only after addition of DBU), along with the peak of H_2 at 4.5 ppm. No peaks were observed in the hydride region to –20 ppm. The pyridine peaks remain essentially unchanged.

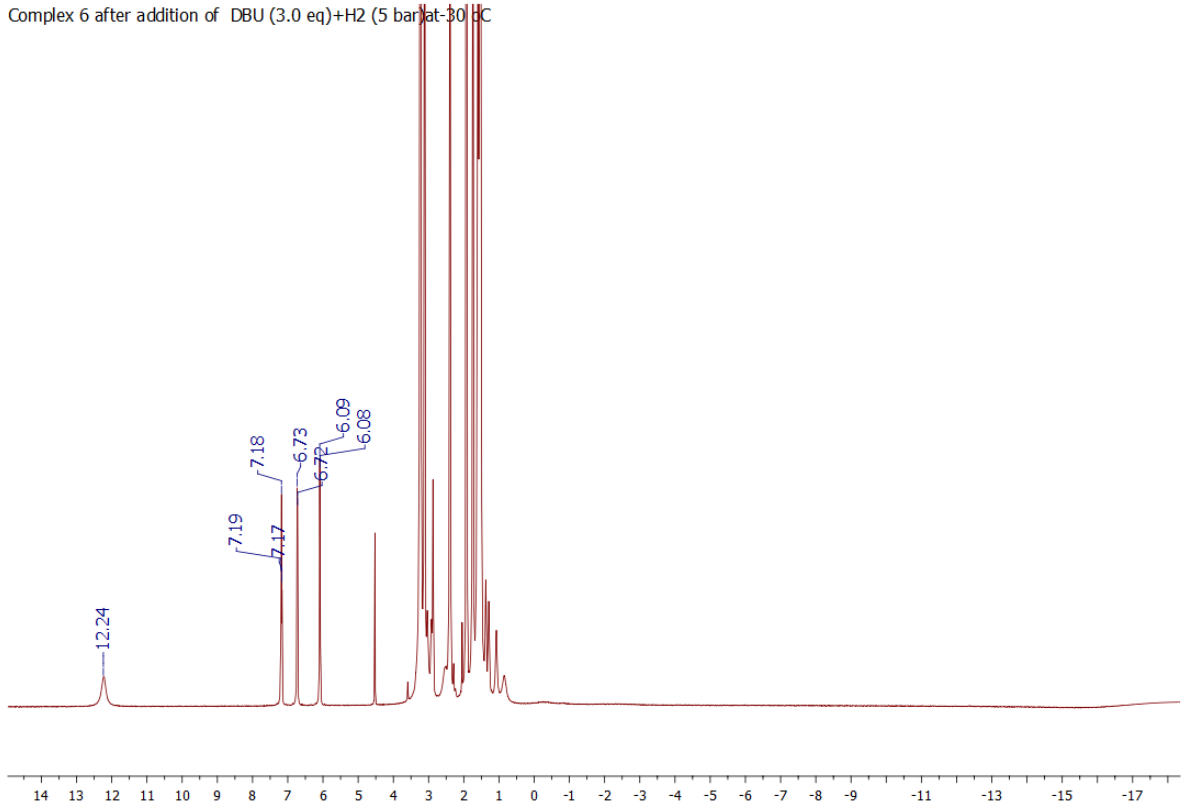

Figure S2. ^1H NMR spectrum of complex **6** after reaction with DBU and H_2 (5 bar) in CD_3CN (-30 °C).

Reactivity of complex 6 in the presence of DBU and CO_2

A Wilmad pressure NMR tube (medium wall thickness) was charged with 5.6 mg of complex **6** in 0.5 mL of CD_3CN. Then 3.0 equiv of DBU were added. The NMR tube was pressurized to 5 bar pressure using CO_2. An NMR spectrum was recorded at -30 °C. NMR spectrum was recorded again at -30 °C showing pyridyl multiplets at 6.09, 6.73 and 7.18 ppm, essentially at the same positions as in the solution of in the presence of DBU only (without CO_2); the broad singlet shifts to 12.7 ppm after addition of CO_2, as compared to a broad peak at 12.3 ppm observed before addition of CO_2 gas (Figure S3).

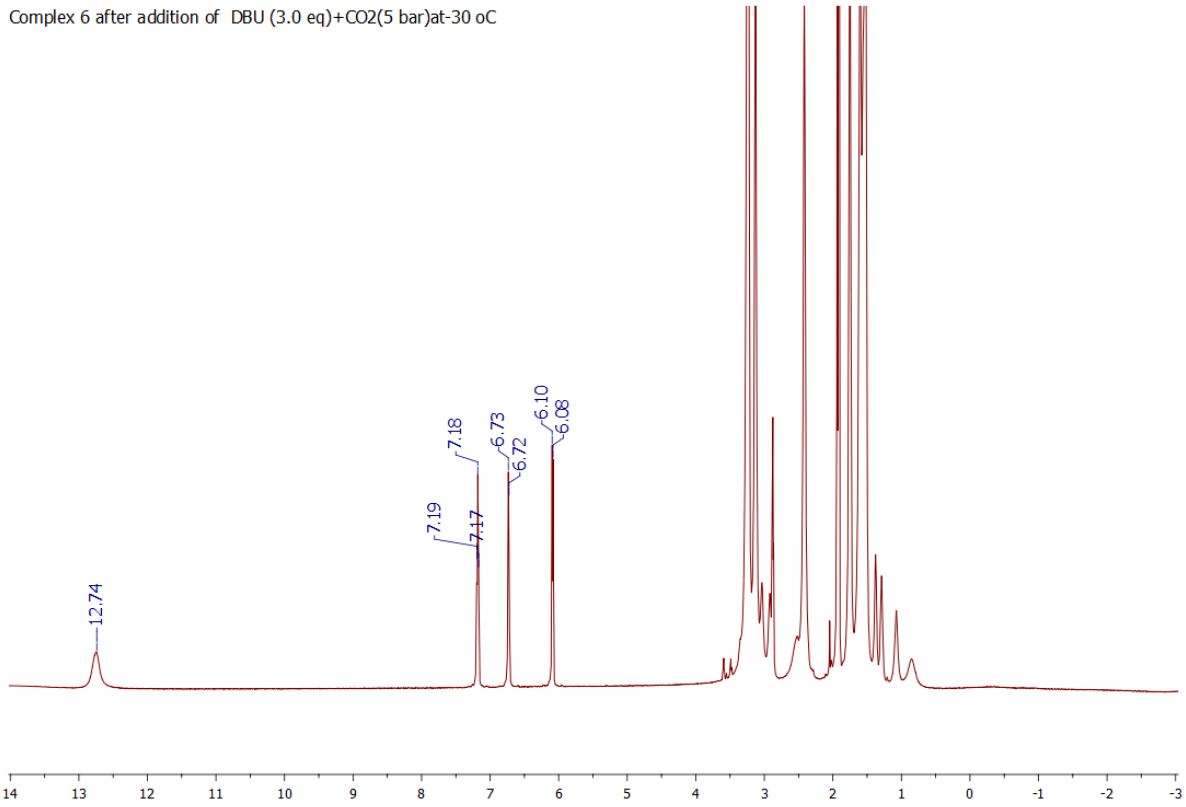

Figure S3. ^{1}H NMR spectrum of complex **6** after reaction with DBU and CO_2 (5 bar) in CD_3CN (-30 °C).

Reactivity of complex 6 in the presence of DBU and H_2 : CO_2 (1:1) mixture

A Wilmad pressure NMR tube (medium wall thickness) was charged with 5.6 mg of complex **6** in 0.5 mL of CD_3CN. Then 3.0 equiv of DBU were added. The NMR tube was pressurized to 5 bar pressure using a pre-mixed 1 : 1 mixture of CO_2 and H_2. An NMR spectrum was recorded at RT. The solution was then heated at 50 °C, periodically cooled down to RT, and the changes were followed by ^{1}H NMR during the course of 16 h (Figure S4).

When NMR was recorded at RT immediately after addition of H_2 : CO_2 mixture, the aromatic signals were analogous to those observed upon reaction of complex 6 with DBU only, however, a small intensity peak at ~ –0.9 ppm was observed. After heating at 50 °C and cooling down to RT, the peak at –0.9 ppm persists, however, due to the small intensity of NMR peaks of this minor species, the product could not be characterized. During the reaction, the formate peak (8.55 ppm) intensity steadily increases reaching a TON of 6 after 5 h and a TON of 12 after 16 h. The aromatic peaks of the ligand correspond to peaks of the deprotonated complex **6** during the first 5 hours of reaction (TON 6). However, when excess formate is present after 16h, another species becomes apparent, represented by a singlet at 8.11 ppm and another set of aromatic signals, which could belong to a Mn formate complex. At this point however, the nature of these species and the mechanism of the reaction are under further investigation.

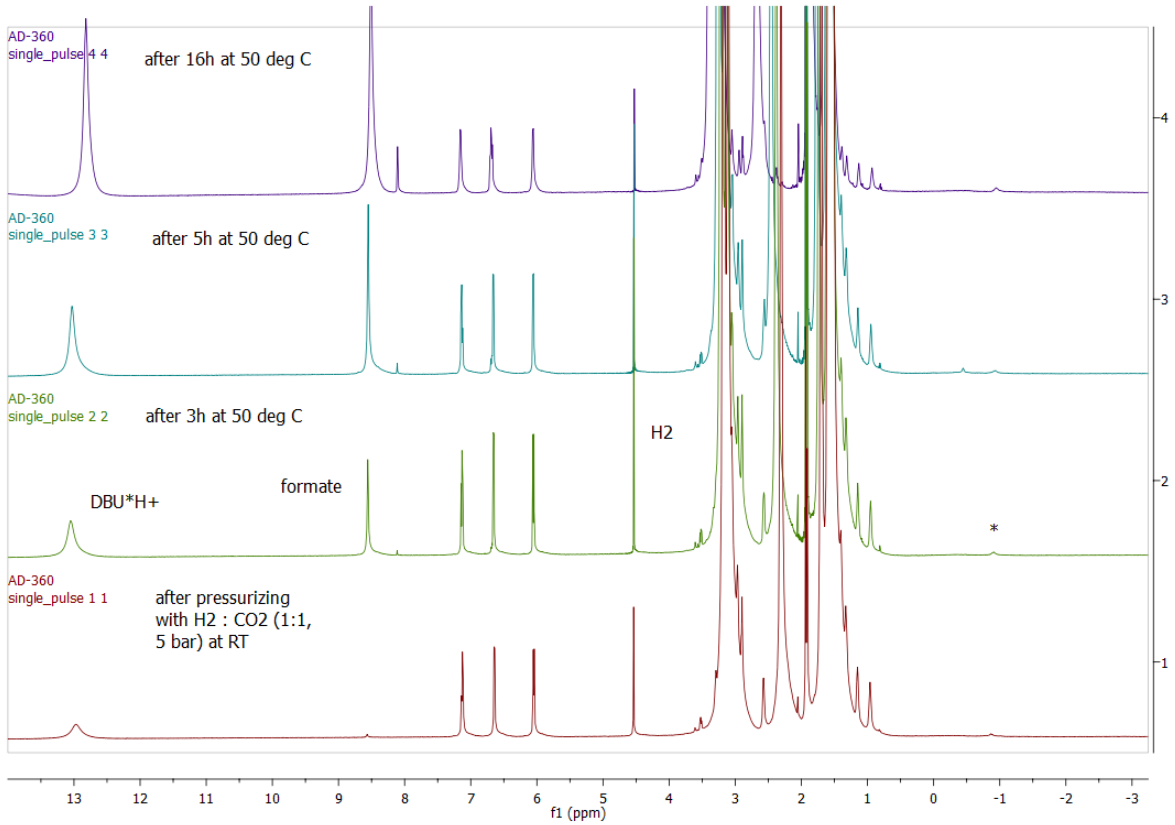

Figure S4. ^{1}H NMR spectrum of complex **6** in the presence of DBU in CD_3CN pressurized with H_2:CO_2 (1:1) mixture (5 bar). The peak marked with an asterisk is a minor species featuring a singlet at -0.9 ppm after addition of the H_2:CO_2 mixture.

Reactivity of complex 2 in the presence of DBU and H_2 : CO_2 (1:1) mixture

A Wilmad pressure NMR tube (medium wall thickness) was charged with 3.8 mg of complex **2** in 0.5 mL of CD_3CN or THF-d_8. Then 3 equiv of DBU were added. The NMR tube was pressurized to 4 bar pressure in CD_3CN using a pre-mixed 1 : 1 mixture of CO_2 and H_2. The NMR spectrum was recorded at RT. The the solution was then heated at 50 °C, periodically cooled down to RT, and the changes were followed by ^{1}H NMR during the course of 2-18 h. NMR shows broadening of the signals and formation of a complex mixture of bipyridine-containing compounds, while no formate is detected. After addition of H_2-CO_2 mixture, the color changed to dark brown after 2 h. The UV-vis spectrum was recorded in MeCN solution after reacting for 2 h in a screw-cap sealed quartz cuvette (10 mm pathlength) showing absorption bands at 810, 634, and 390 nm. These bands are consistent with the spectrum of the Mn(0) dimer $(bipy)_2Mn_2(CO)_6$ reported in the literature for an MeCN solution.[1] The UV-vis spectrum is shown in Figure S5.

The analogous reaction in THF also yields a dark colored solution, which shows the presence of several bipyridine-containing species in solution.

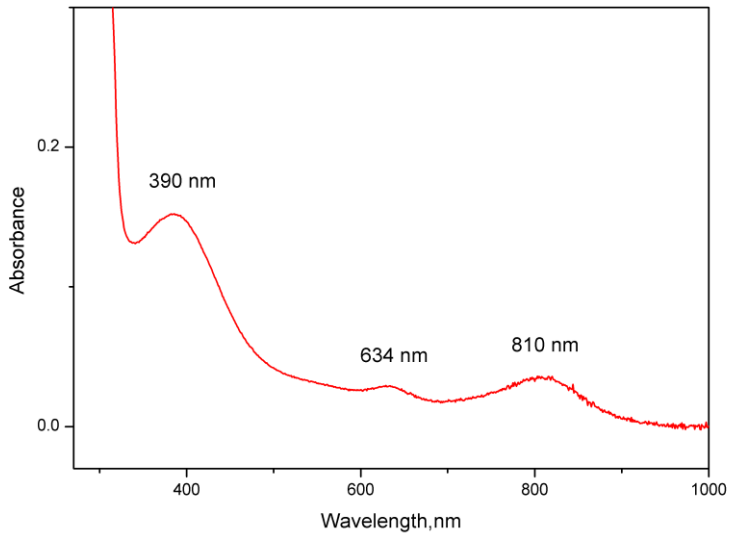

Figure S5. UV-vis spectrum of the reaction mixture containing complex **2**, DBU in acetonitrile solution after heating for 2h under H_2:CO_2 (1:1, 5 bar).

UV-vis and FT-IR changes accompanying the reactivity of complex 6 with DBU.

Changes in the UV-vis spectrum of 6 upon addition of DBU to MeCN solution.

A 2 mL of $9.7*10^{-5}$ M solution of **6** in MeCN was placed into a quartz cuvette (1 cm pathlength). A prepared stock solution of DBU in MeCN was added in portions of 100 µL, each containing 1 equiv of DBU relative to Mn complex. After addition of 2 equiv of DBU, the spectrum remains essentially unchanged when subsequently the amount of DBU is increased further to 3 or 4 equivalents. (Figure S6).

The initial spectrum in the absence of DBU features two absorption bands at 329 and 343 nm that can be assigned as MLCT from the Mn center to the 6,6'-dihydroxy-2,2'-bipyridyl ligand. Upon addition of 1 equiv of DBU, the bands shifts and a new feature appears with several peaks at ~350 nm (shoulder), 374 nm, 390 nm and 412 nm. After addition of 2 and more equiv of DBU (up to 4 equiv), absorption bands are present at 390 nm and 412 nm.

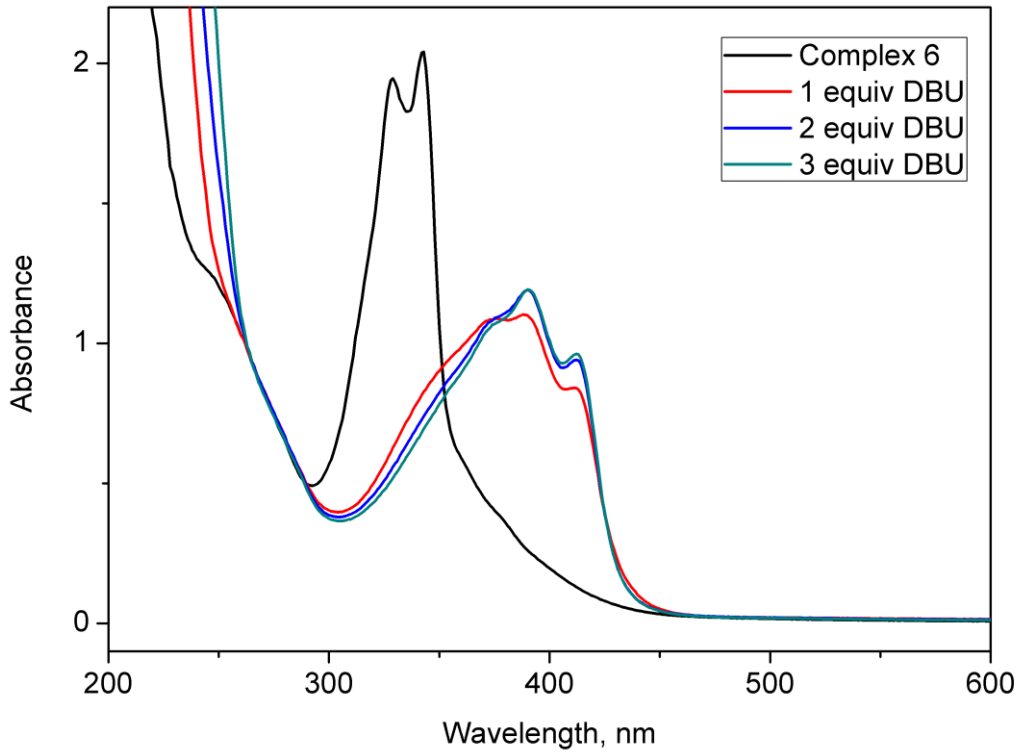

Figure S6. UV-vis spectra of the solution of complex **6** in the absence (black) and in the presence of variable amounts of DBU (1 equiv of DBU relative to **6** – red; 2 equiv – blue; 3 equiv – green).

Changes in the FT-IR spectrum of 6 upon addition of DBU to MeCN or THF solution.

9.0 mg of complex **6** was dissolved in 1.5 mL of MeCN and the solution was divided into three 0.5 mL aliquots.

The FT-IR spectrum was collected first for the solution of **6** without DBU. Two bands are originally present, a sharp band at 2044 cm^{-1} and a broad band at 1947 cm^{-1} that could be assigned to the coordinated nitrile and carbonyl groups (the peaks of carbonyls could not be resolved – see the IR spectrum of **6** in the solid state showing two closely overlapping peaks in the carbonyl stretch region) .

3 equiv of DBU was added to the aliquot of **6**/MeCN solution, and the resulting solution was analyzed by FT-IR. The stretching bands shift to 2002 cm^{-1} and 1888 cm^{-1} (broad).

With another aliquot, 6 equiv of DBU was added, and the solution was once again analyzed by FT-IR. The spectrum remains essentially unchanged when compared to the previous one taken in the presence of 3 equiv of DBU. (Figure S7)

The analogous procedure was used to measure FT-IR changes in solution of **6** in THF upon addition of 3 equiv of DBU (Figure S8).

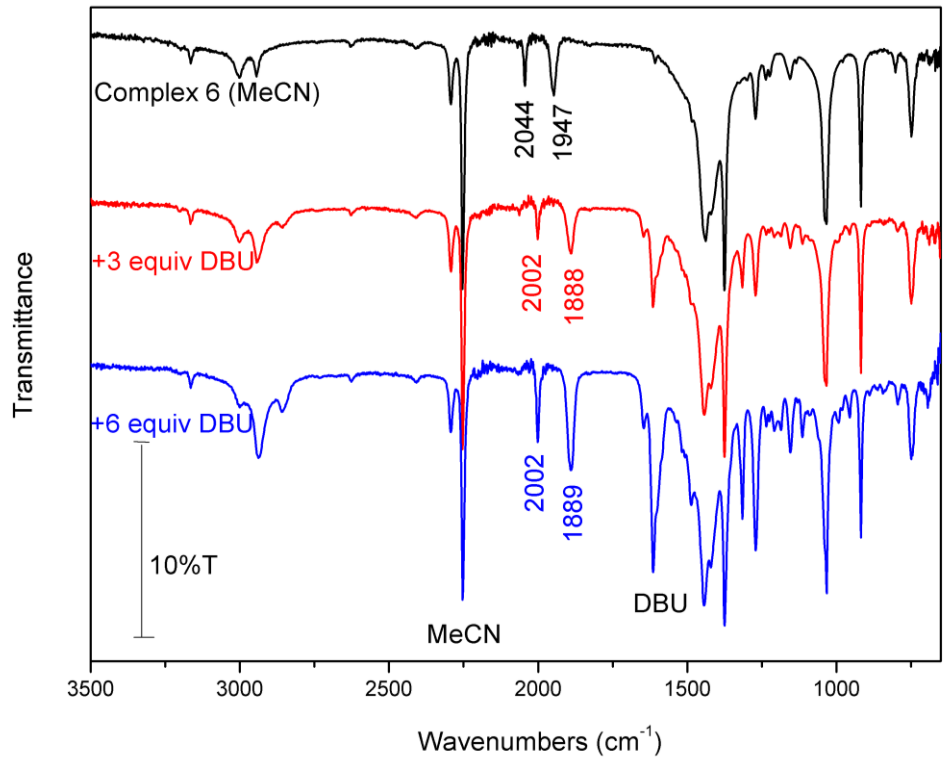

Figure S7. FT-IR spectrum of MeCN solution of complex **6** before addition of DBU (black), after addition of 3 equiv of DBU (red) and after addition of 6 equiv of DBU (blue) (the spectra on the presence of DBU is shifted along the Y-axis).

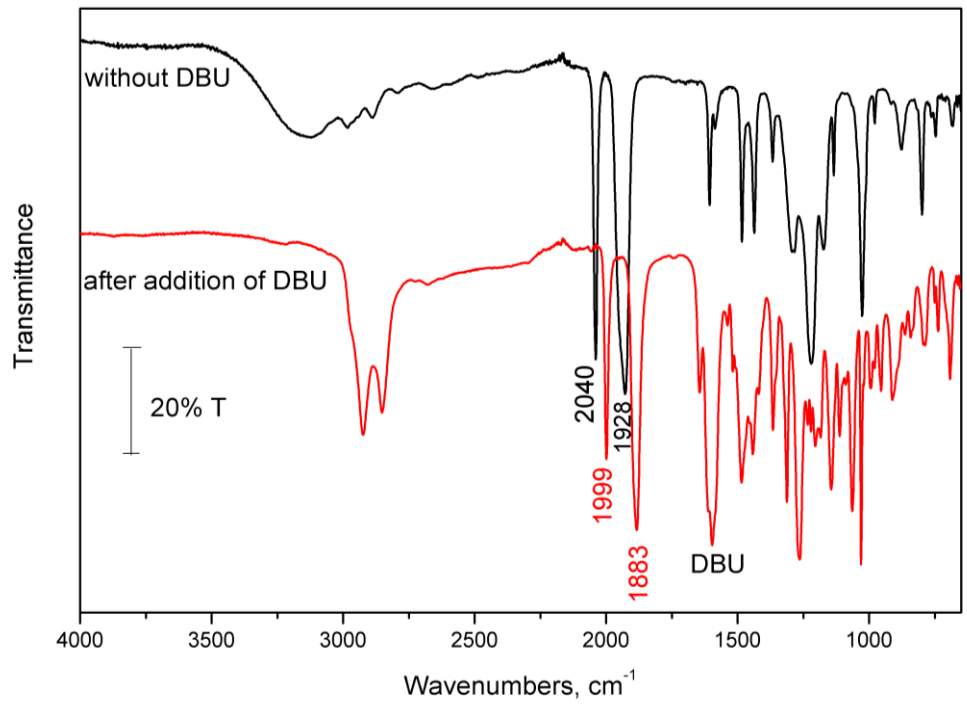

Figure S8. FT-IR spectrum of THF solution of complex **6** before addition of DBU (black) and after addition of DBU (red) (the spectrum on the presence of DBU is shifted along the Y-axis).

NMR spectra of complexes

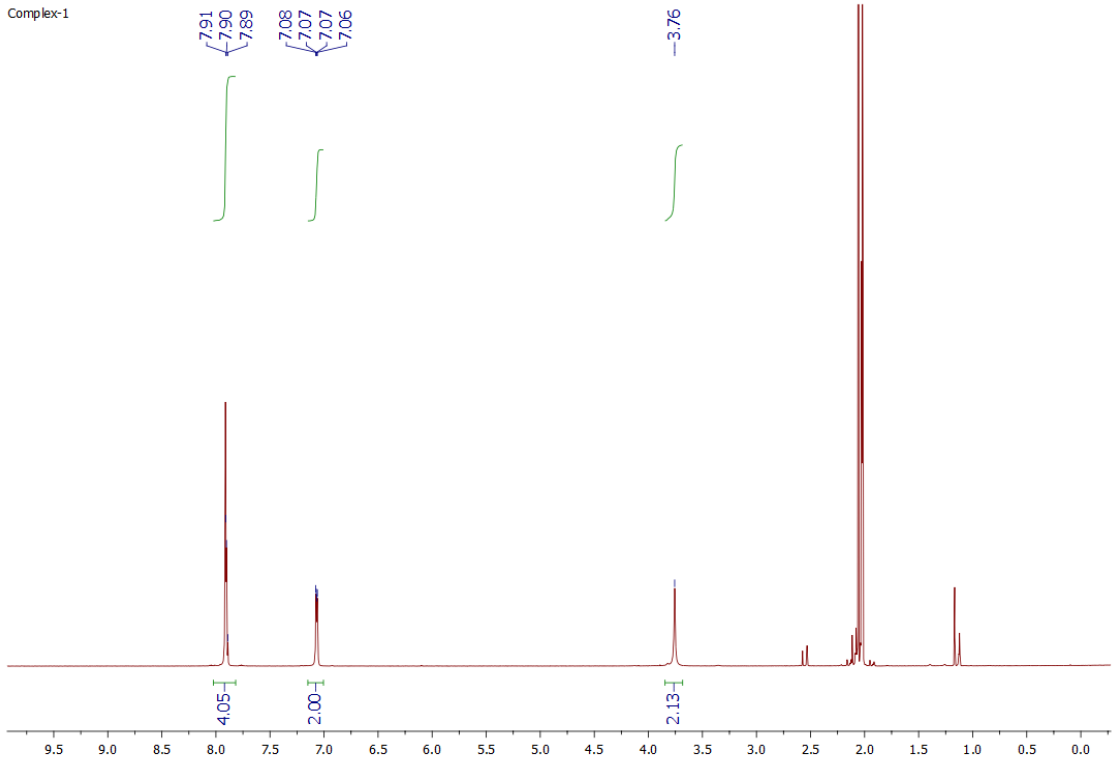

Figure S9. ^{1}H NMR spectrum of **1** in acetone-d_6 at 23 ^{o}C.

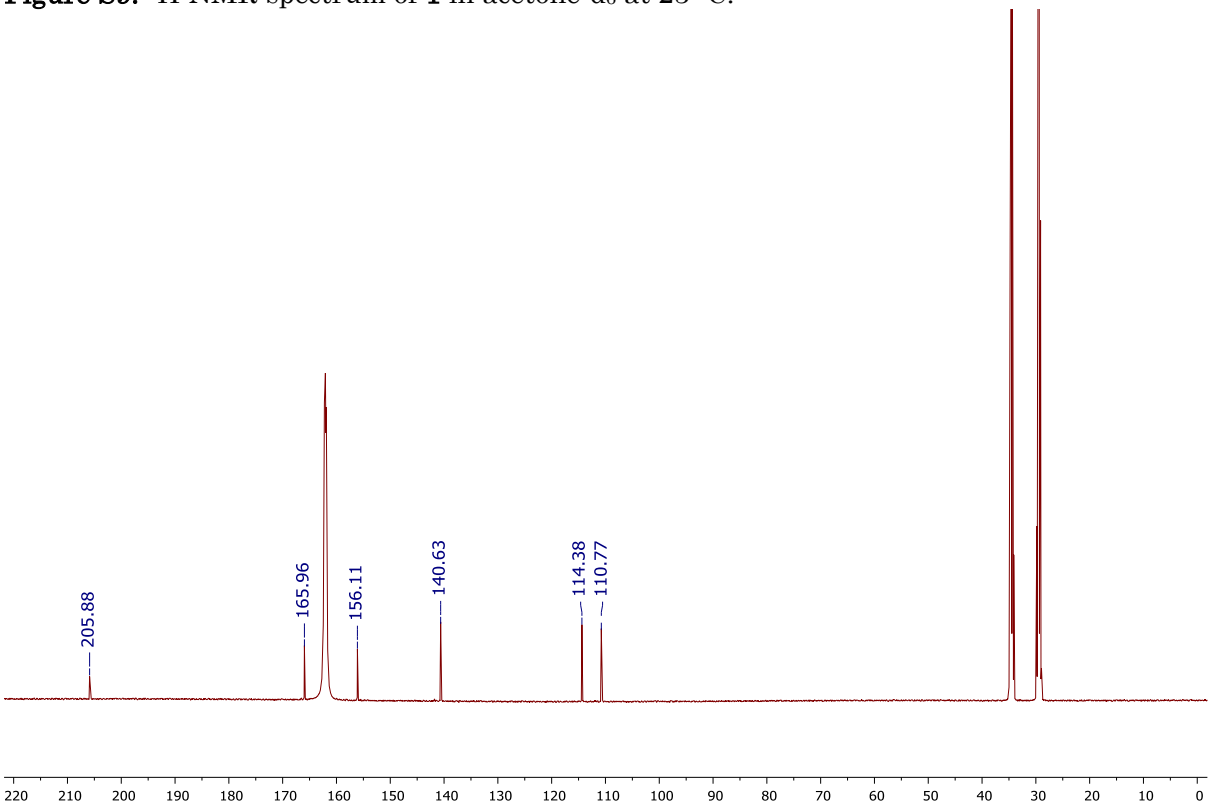

Figure S10. ^{13}C NMR spectrum of **1** in DMF-d_7 at 23 ^{o}C.

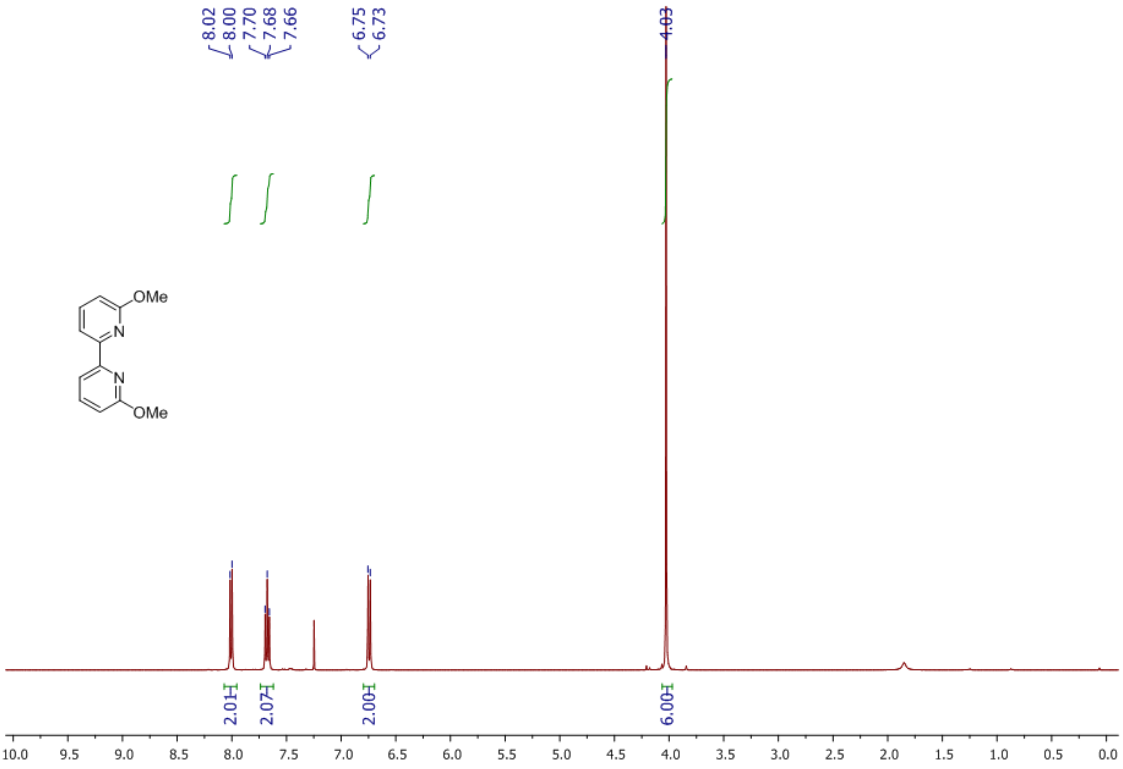

Figure S11. ^{1}H NMR spectrum of 6,6'-dimethoxy-2,2'-bipyridine in $CDCl_3$ at 23 °C.

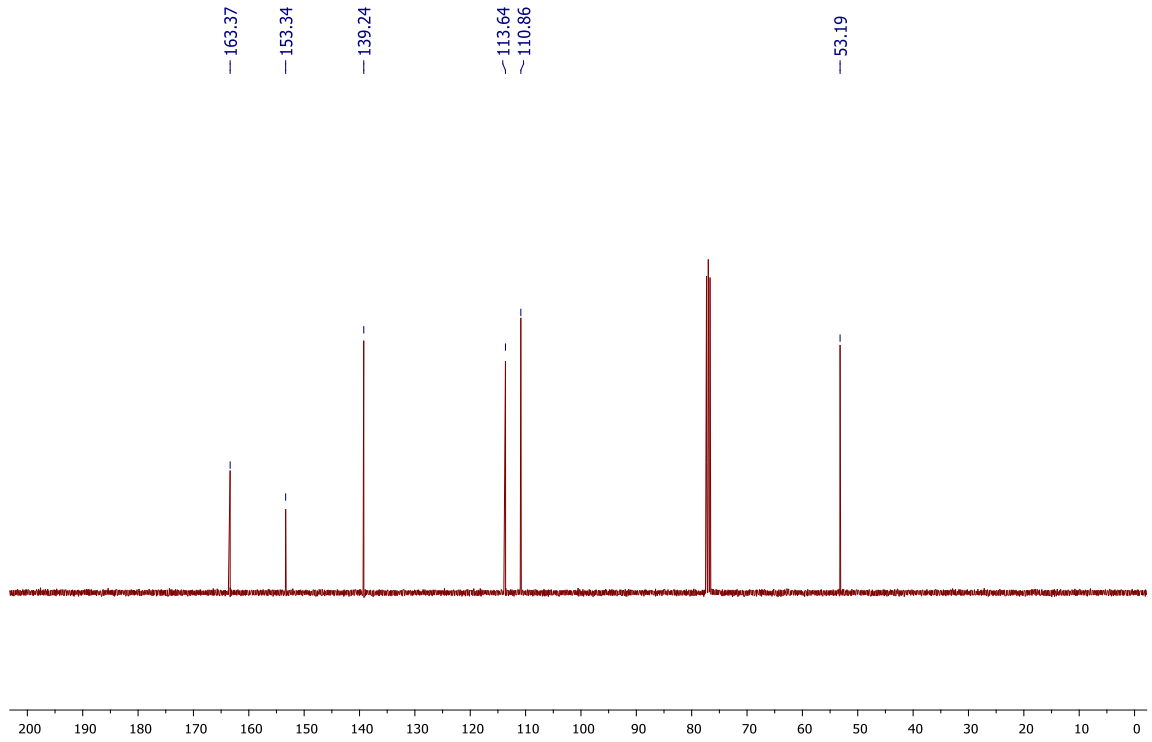

Figure S12. ^{13}C NMR spectrum of 6,6'-dimethoxy-2,2'-bipyridine in $CDCl_3$ at 23 °C.

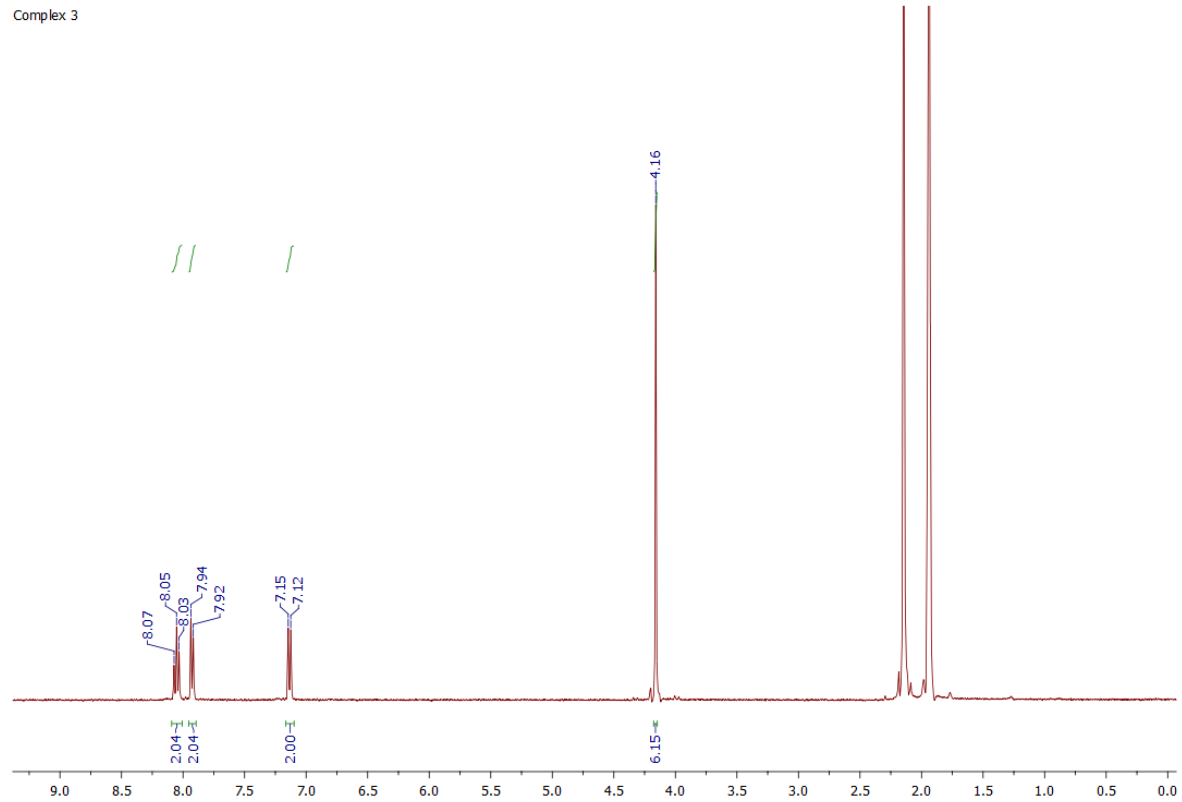

Figure S13. ^{1}H NMR spectrum of **3**, acetone-d_6 at 23 ^{o}C.

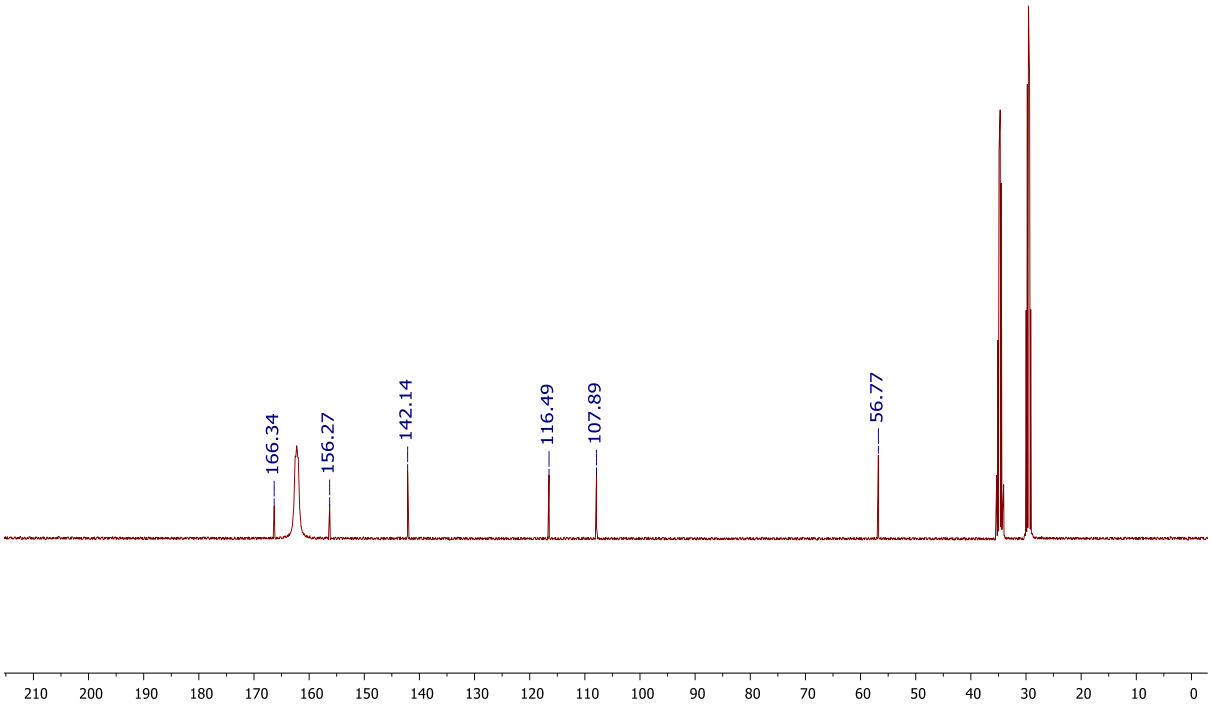

Figure S14. ^{13}C NMR spectrum of **3** in DMF-d_7 at 23 ^{o}C. Carbonyl peaks could not be detected due to broadening of the peaks and low intensity.

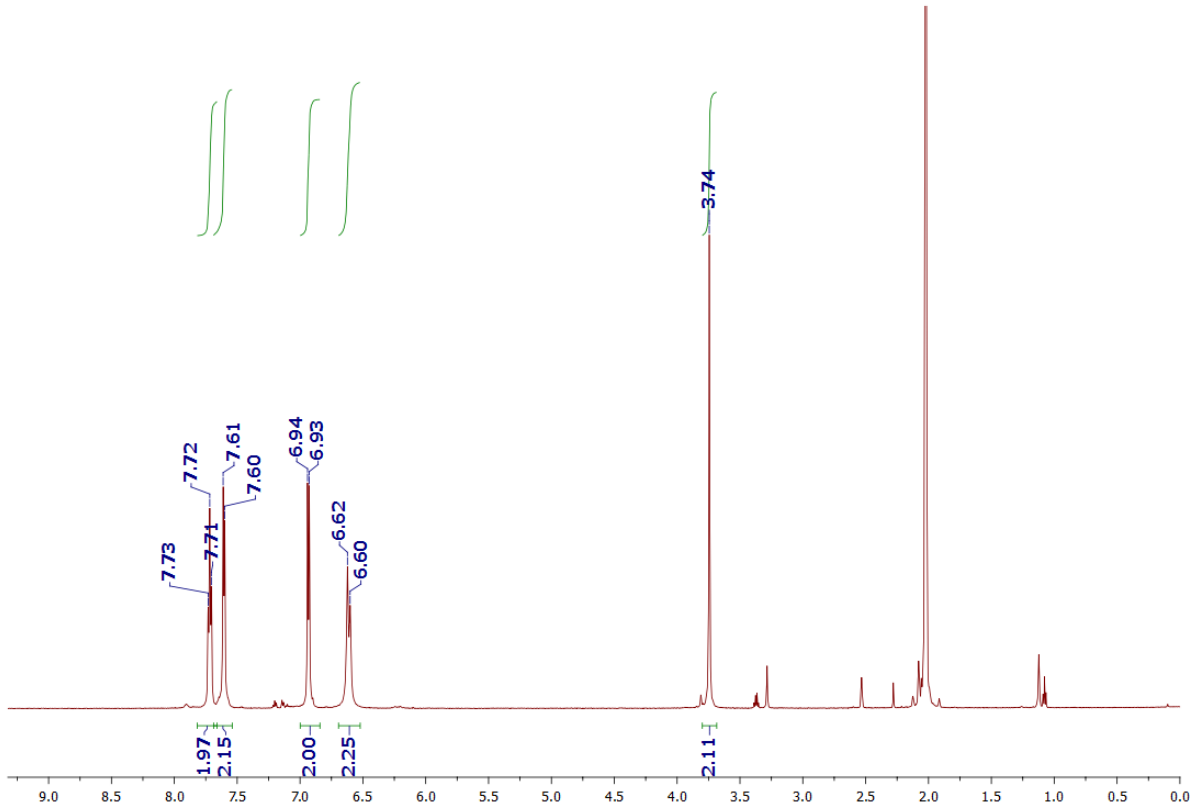

Figure S15. ^{1}H NMR spectrum of **4** in acetone-d_6 at 23 ^{o}C.

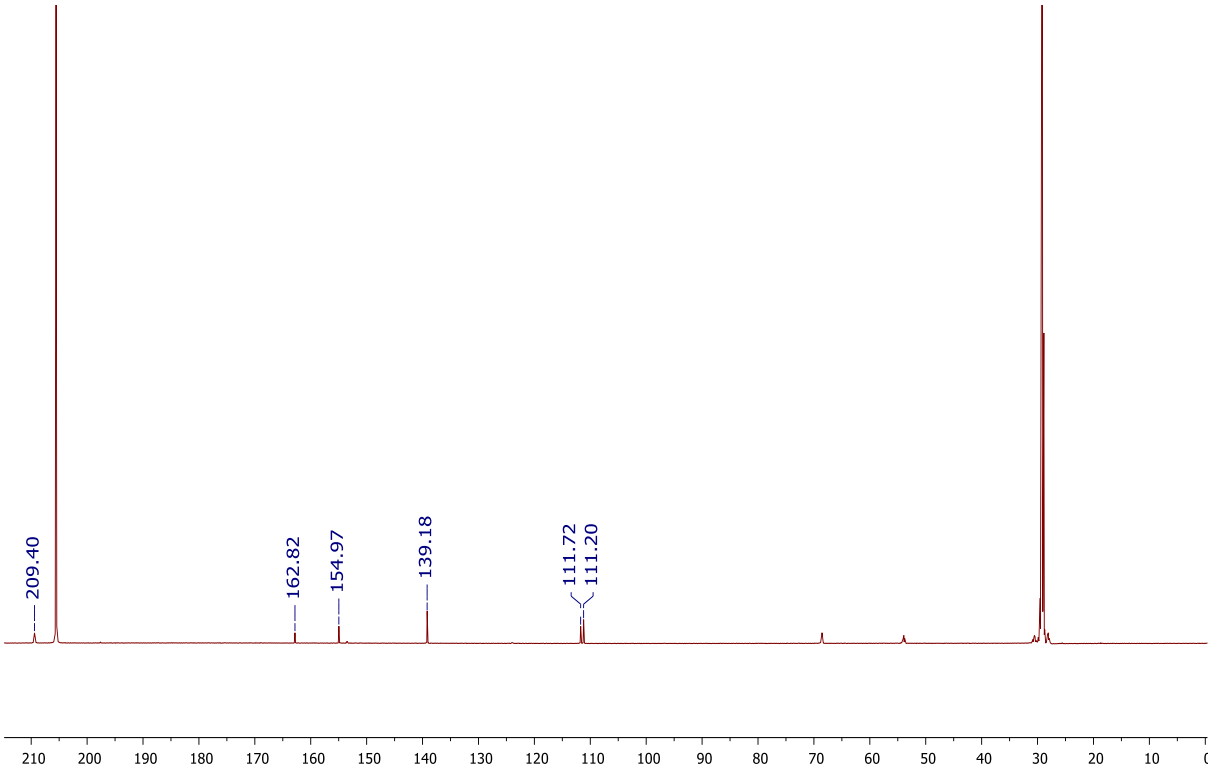

Figure S16. ^{13}C NMR spectrum of **4** in acetone-d_6 at 23 ^{o}C.

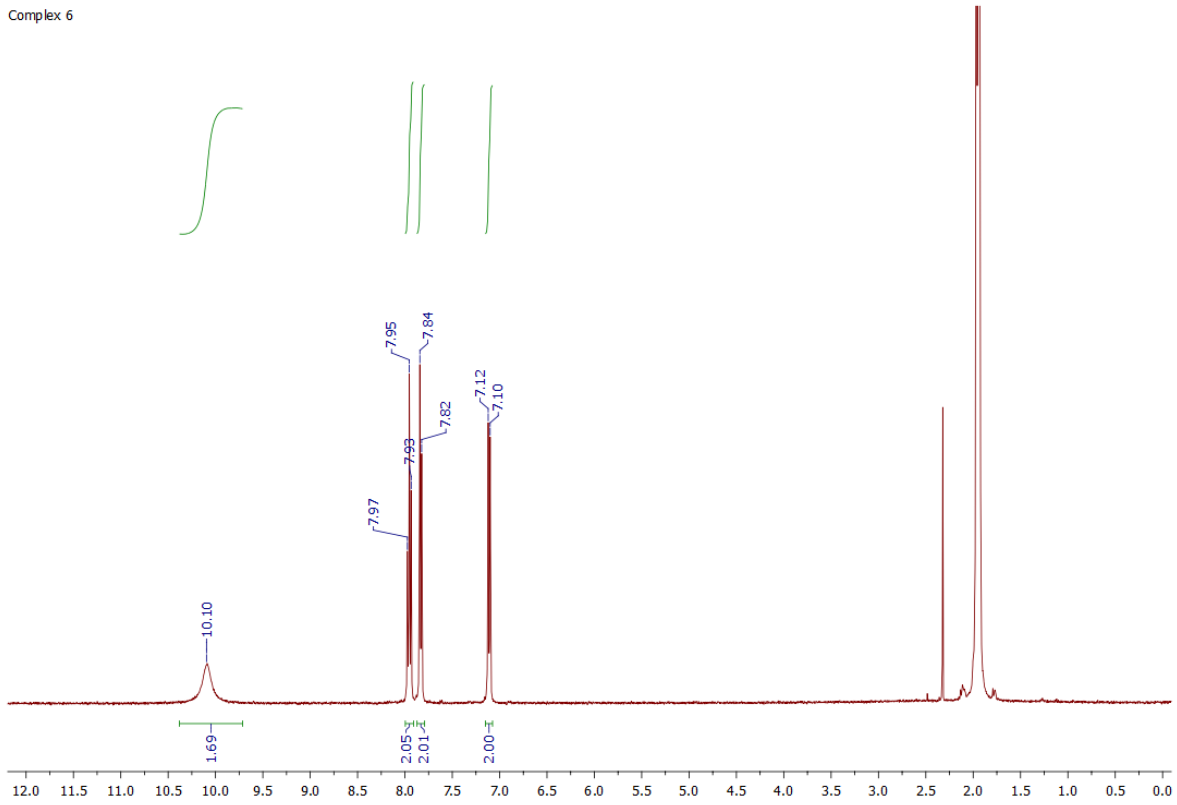

Figure S17. ^{1}H NMR spectrum of **6** in acetonitrile-d_3 at 23 ^{o}C.

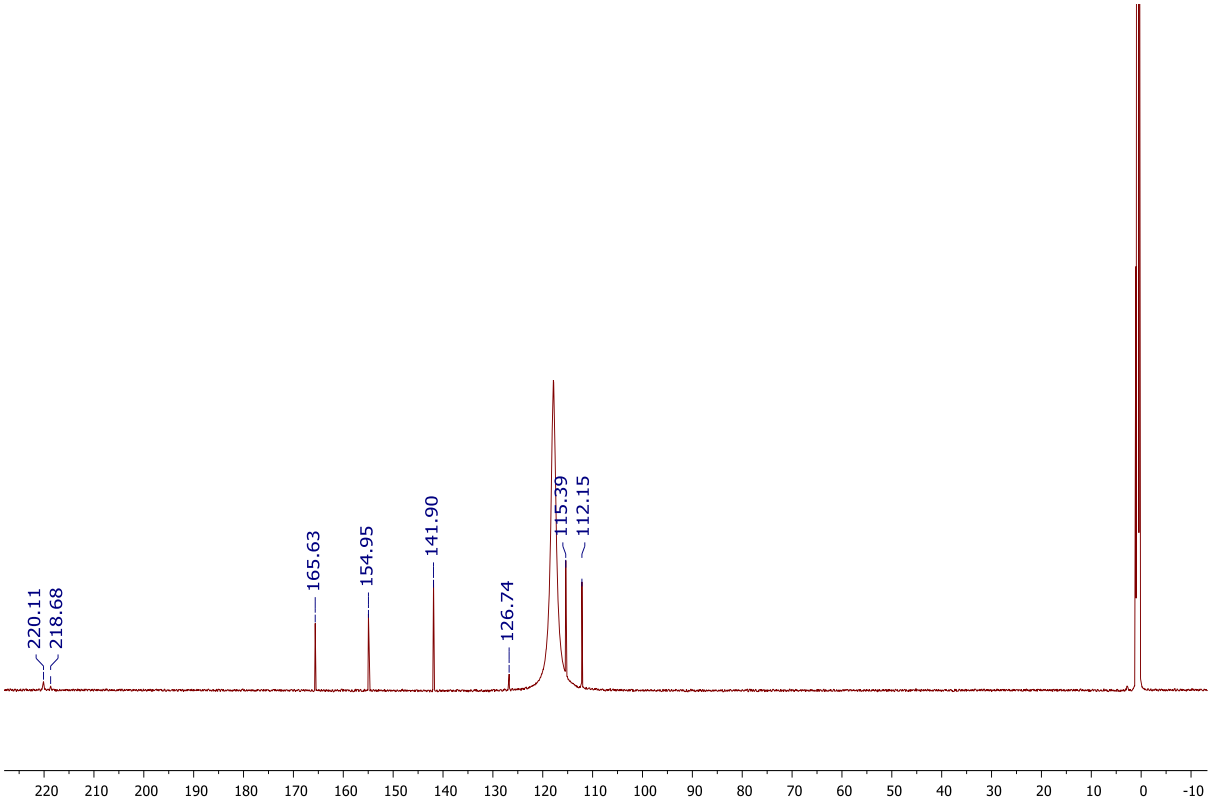

Figure S18. ^{13}C NMR spectrum of **6** in acetonitrile-d_3 at -30 ^{o}C.

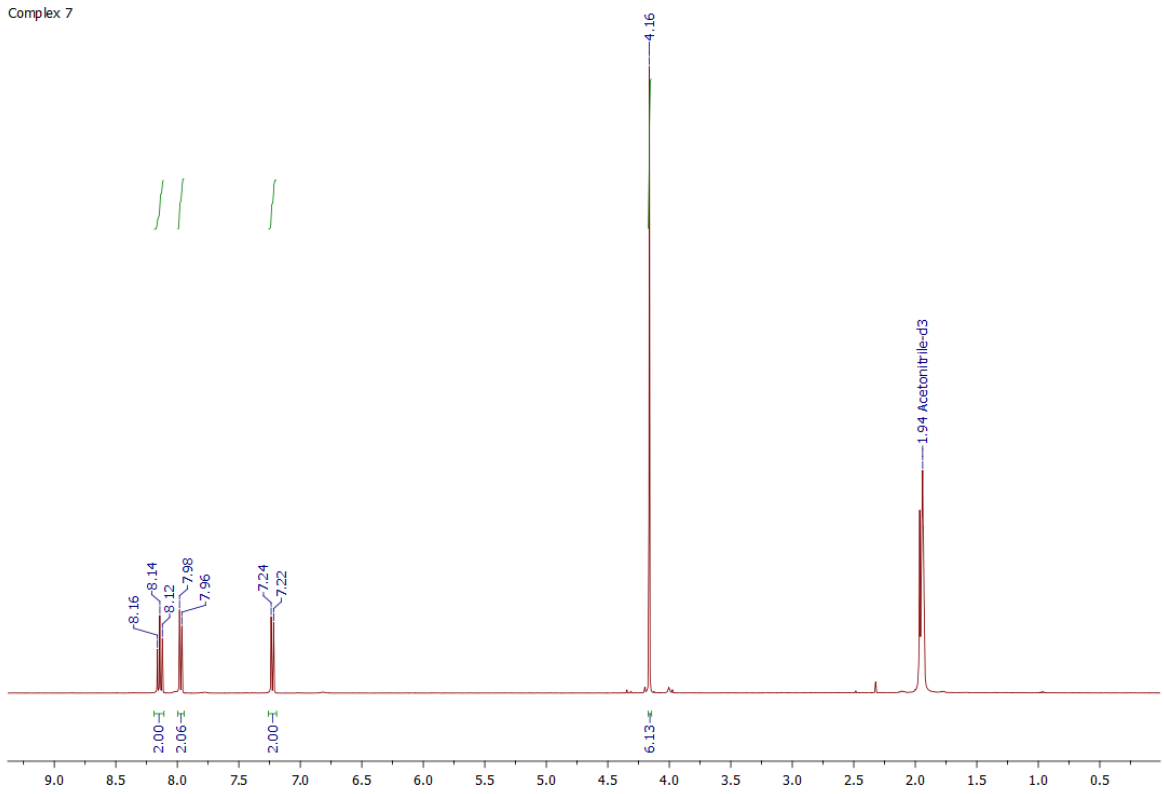

Figure S19. ^{1}H NMR spectrum of **7** in acetonitrile-d_3 at 23 °C.

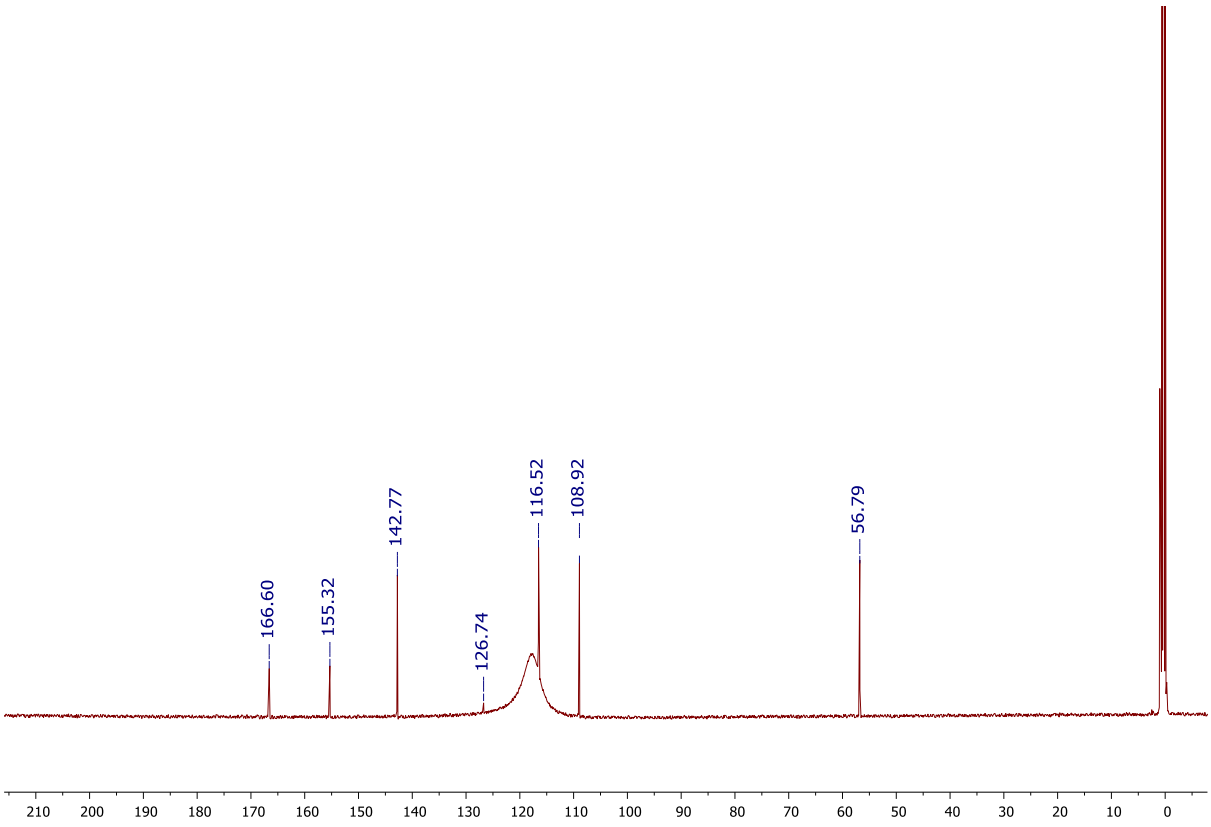

Figure S20. ^{13}C NMR spectrum of **7** in acetonitrile-d_3 at 23 °C.

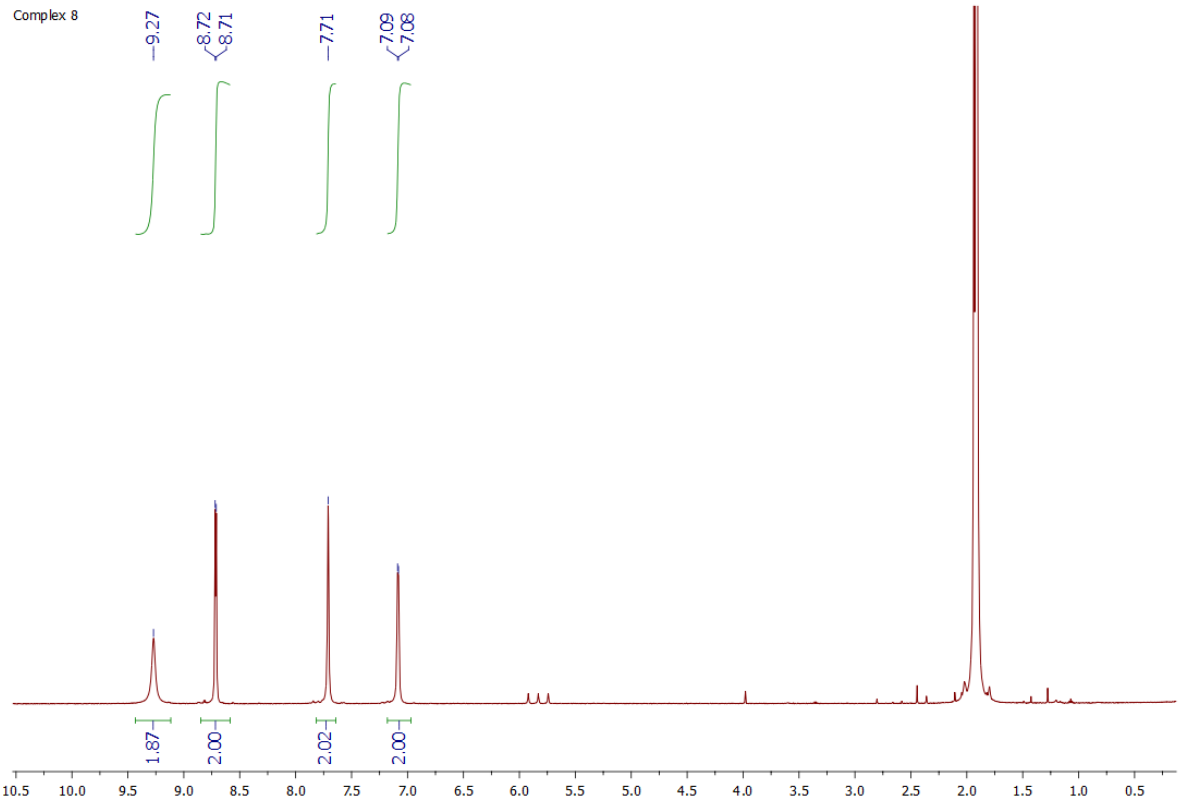

Figure S21. ^{1}H NMR spectrum of **8** in acetonitrile-d_3 at -30 °C.

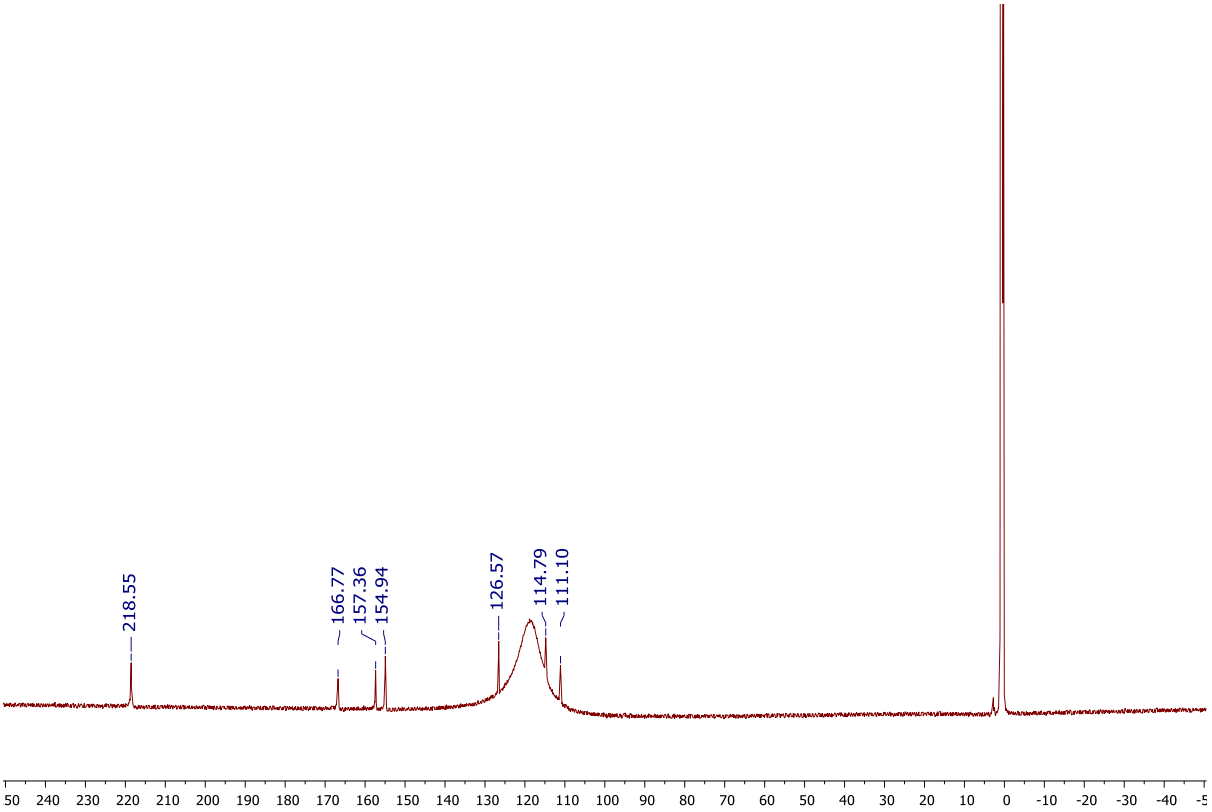

Figure S22. ^{13}C NMR spectrum of **8** in acetonitrile-d_3 at -30 °C.

Representative NMR spectra of the reaction mixtures

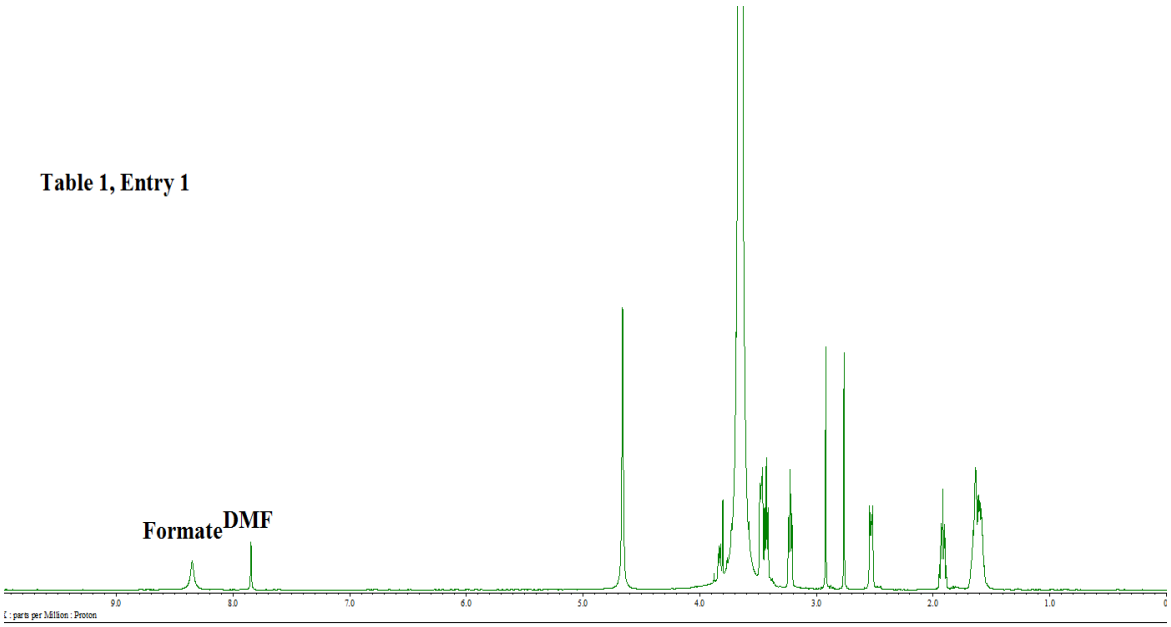

Figure S23. ^{1}H NMR spectrum for the hydrogenation of CO_2 to formate (Table 1, entry 1)

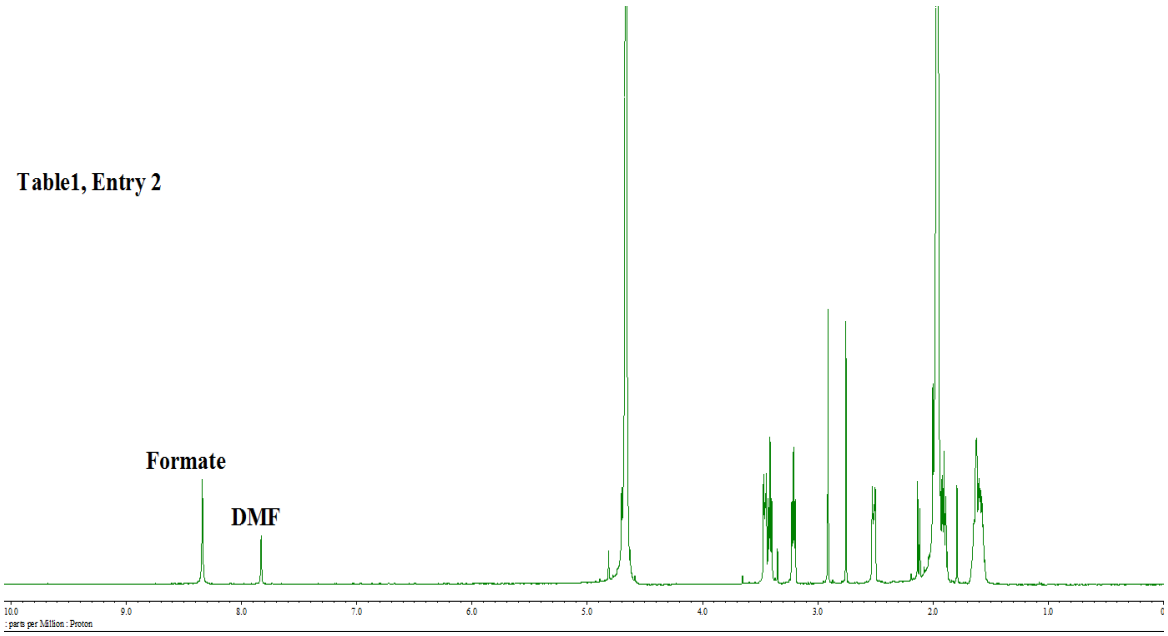

Figure S24. ^{1}H NMR spectrum for the hydrogenation of CO_2 to formate (Table 1, entry 2).

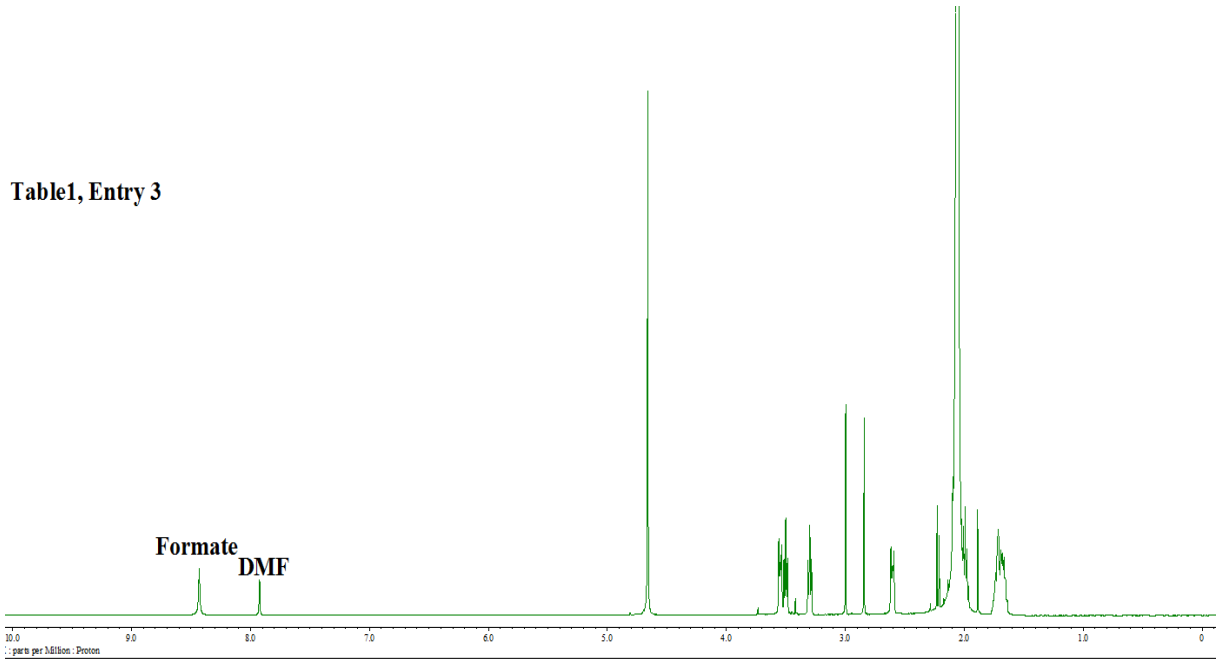

Figure S25. ^{1}H NMR spectrum for the hydrogenation of CO_2 to formate (Table 1, entry 3).

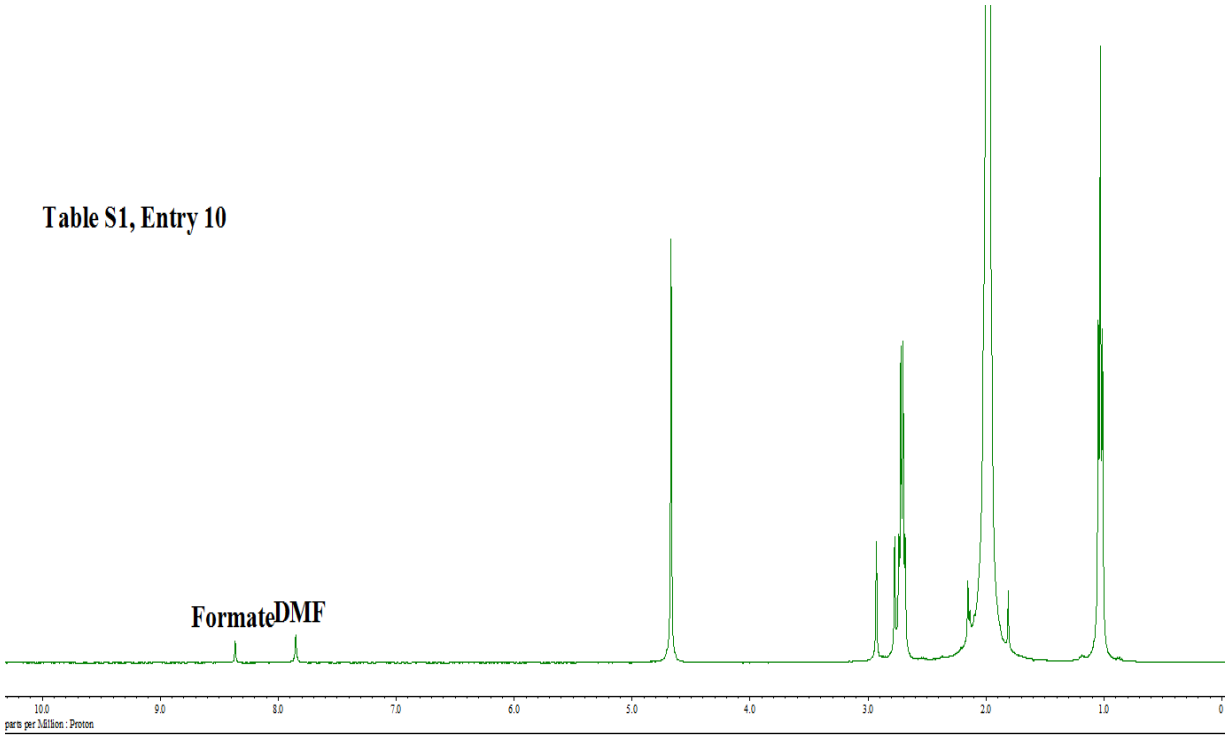

Figure S26. ^{1}H NMR spectrum for the hydrogenation of CO_2 to formate using Et_3N base (Table S1, entry 10).

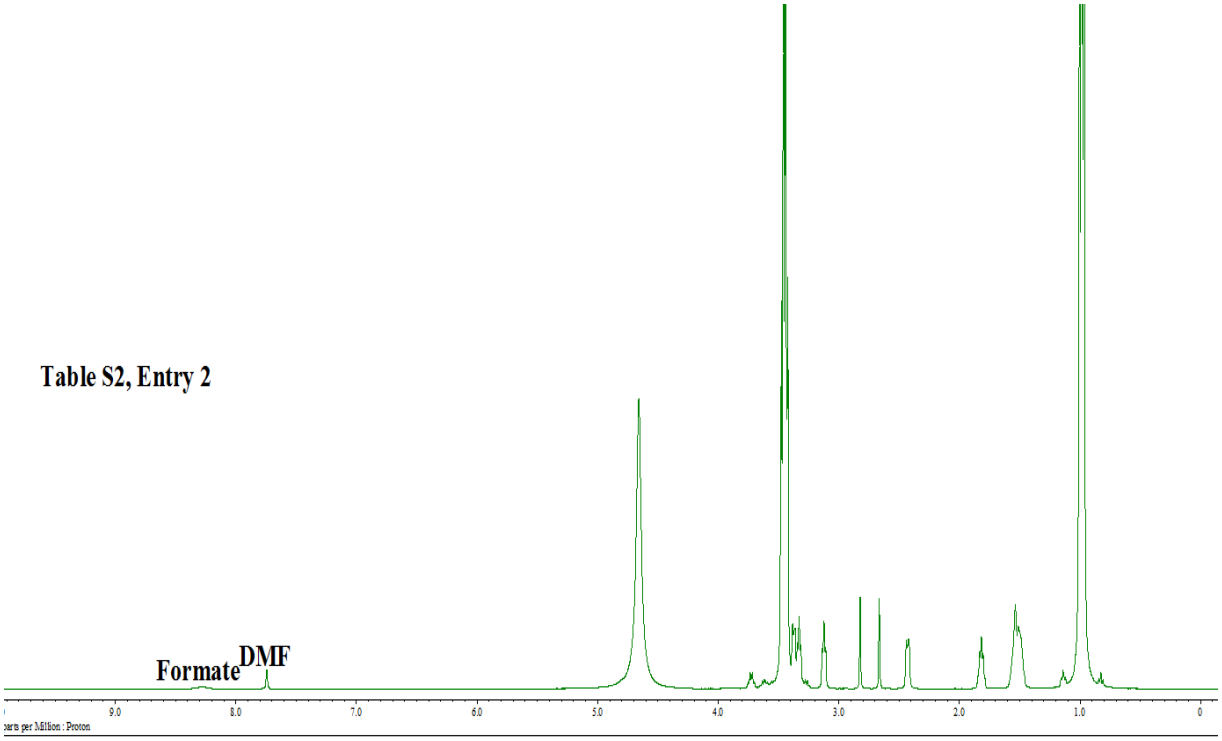

Figure S27. ^{1}H NMR spectrum for the hydrogenation of CO_2 to formate using EtOH as solvent (Table S2, entry 2).

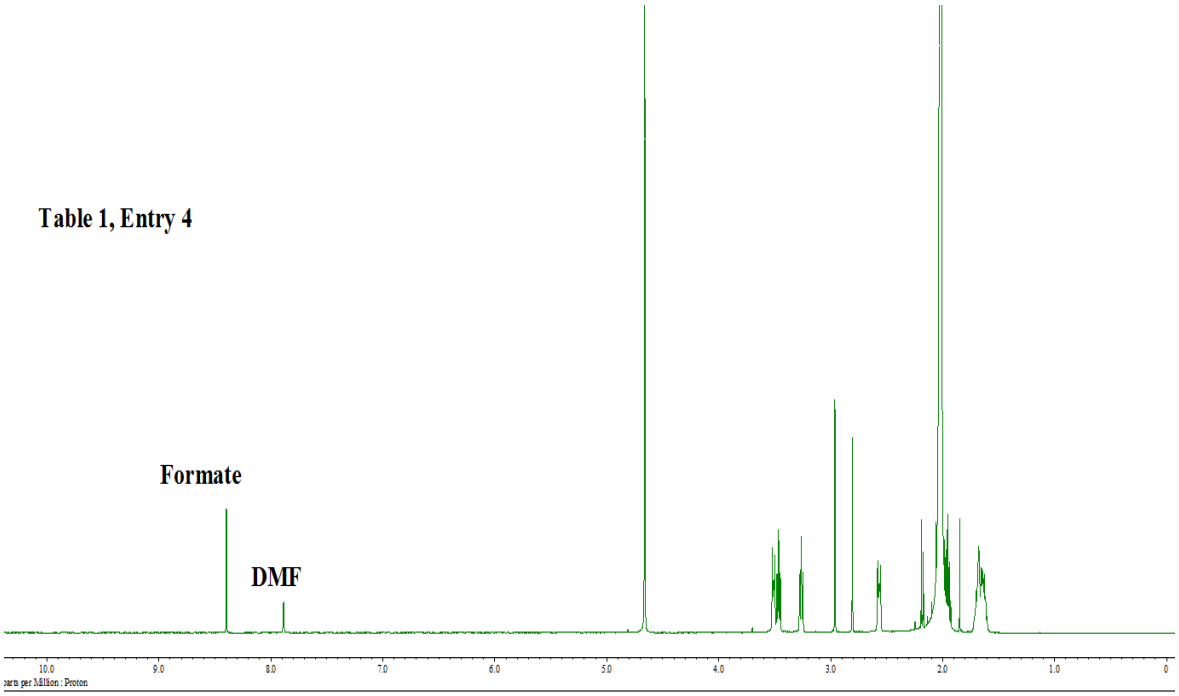

Figure S28. ^{1}H NMR spectrum for the hydrogenation of CO_2 to formate (Table 1, entry 4).

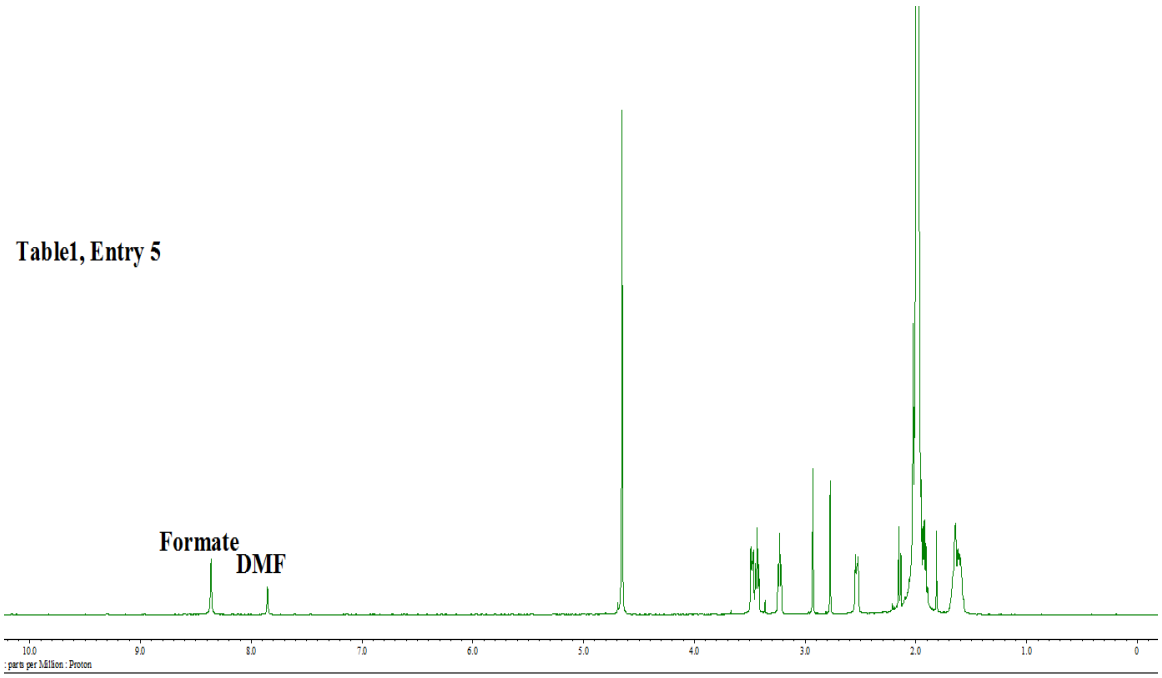

Figure S29. ^{1}H NMR spectrum for the hydrogenation of CO_2 to formate (Table 1, entry 5).

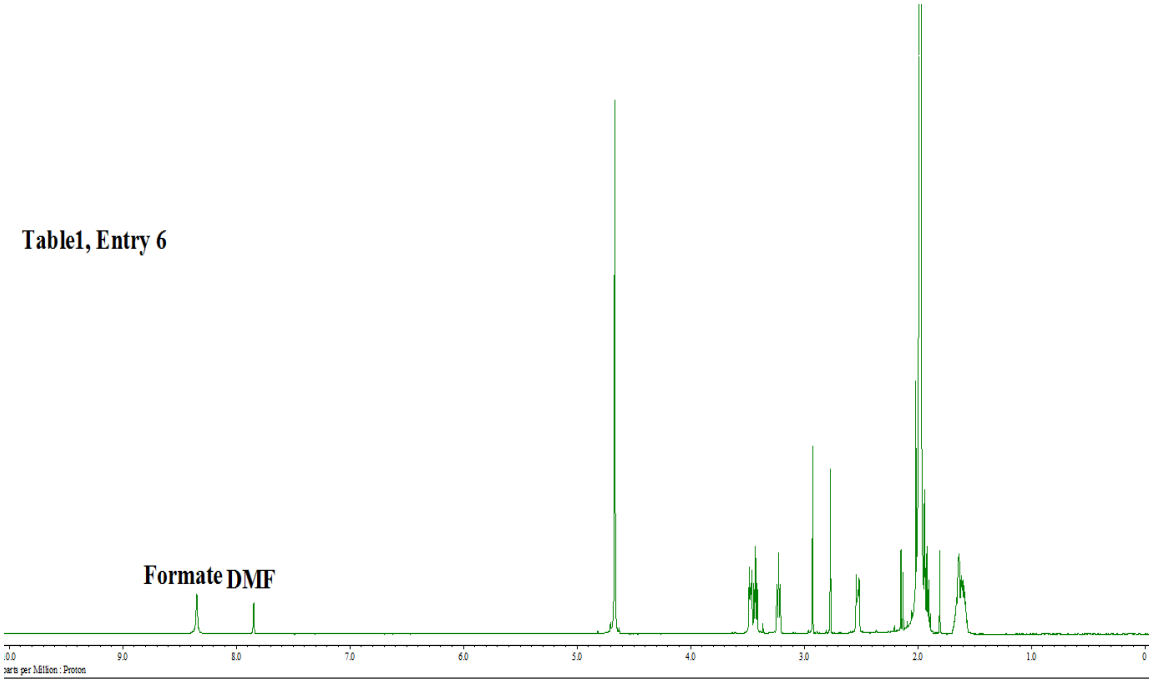

Figure S30. ^{1}H NMR spectrum for the hydrogenation of CO_2 to formate (Table 1, entry 6).

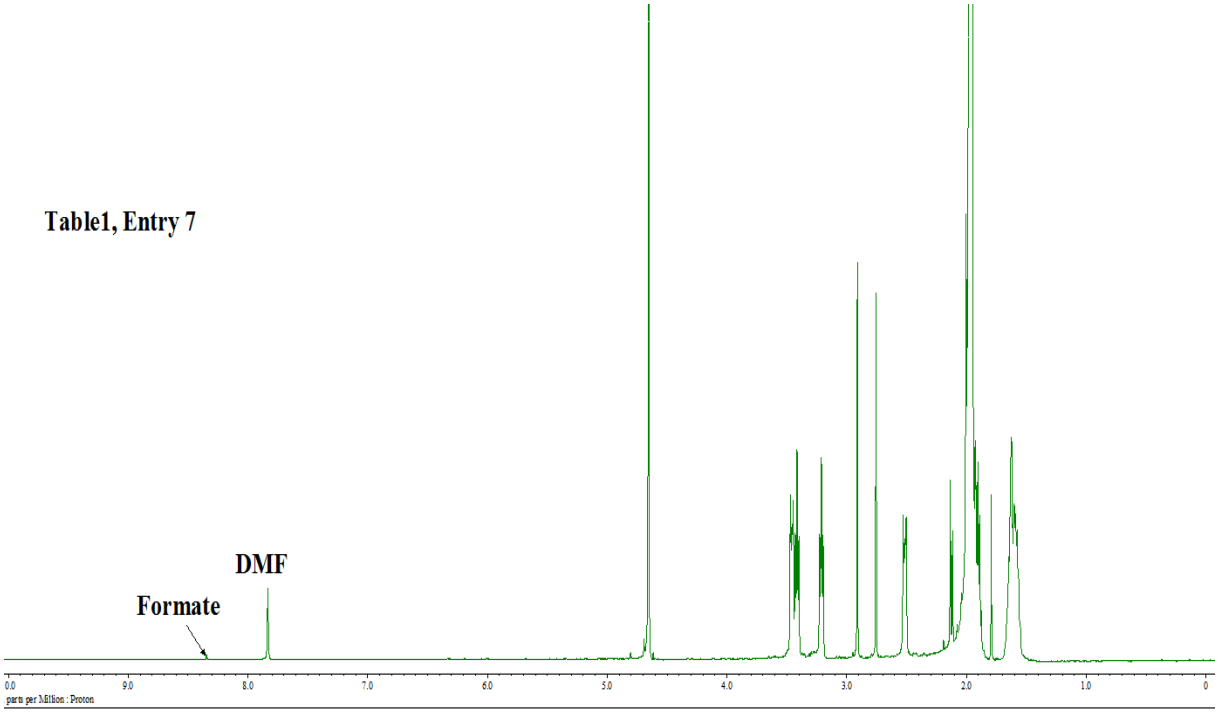

Figure S31. ^{1}H NMR spectrum for the hydrogenation of CO_2 to formate (Table 1, entry 7).

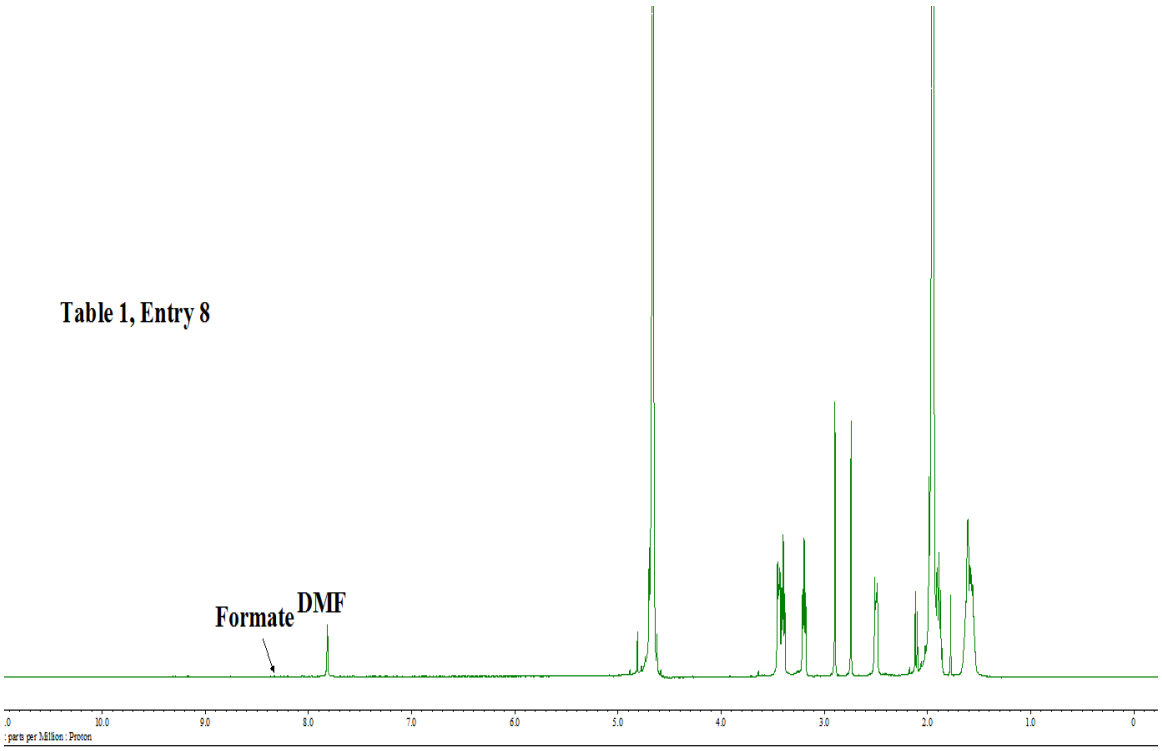

Figure S32. ^{1}H NMR spectrum for the hydrogenation of CO_2 to formate (Table 1, entry 8).

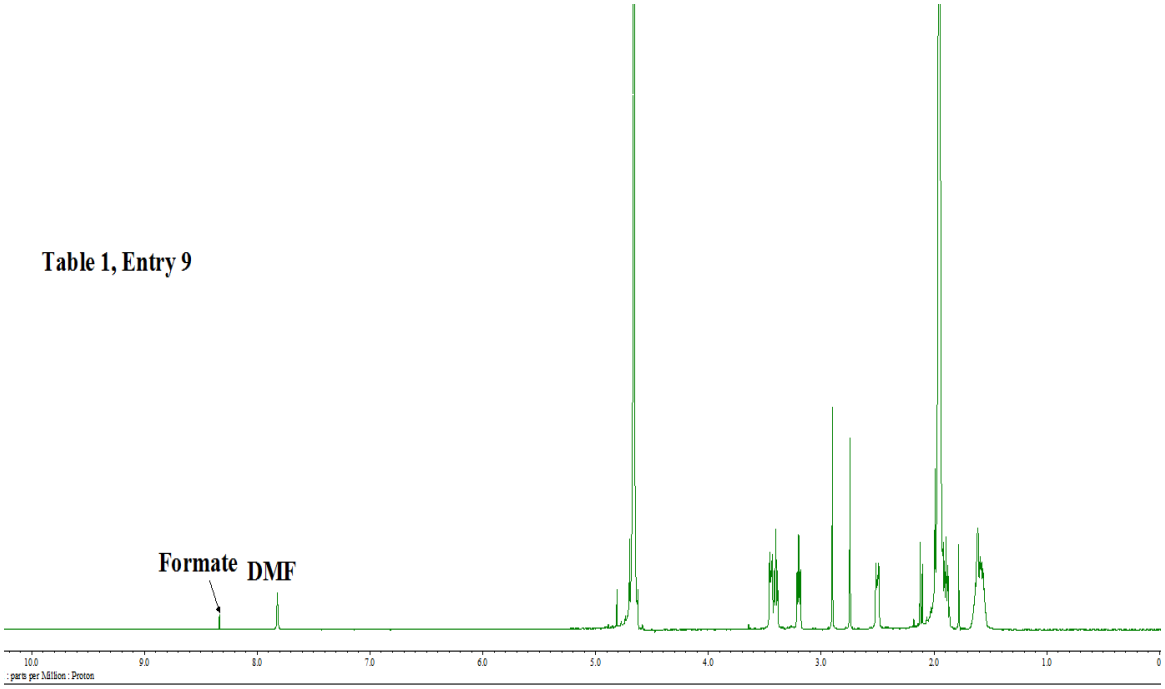

Figure S33. ^{1}H NMR spectrum for the hydrogenation of CO_2 to formate (Table 1, entry 9).

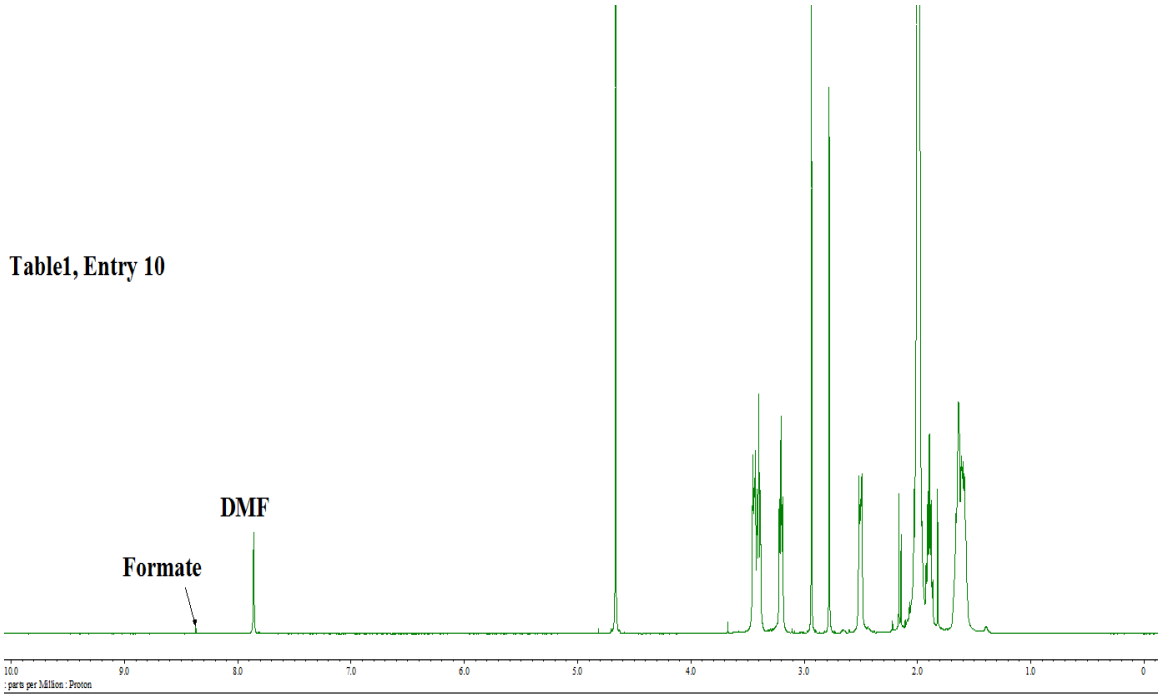

Figure S34. ^{1}H NMR spectrum for the hydrogenation of CO_2 to formate (Table 1, entry 10).

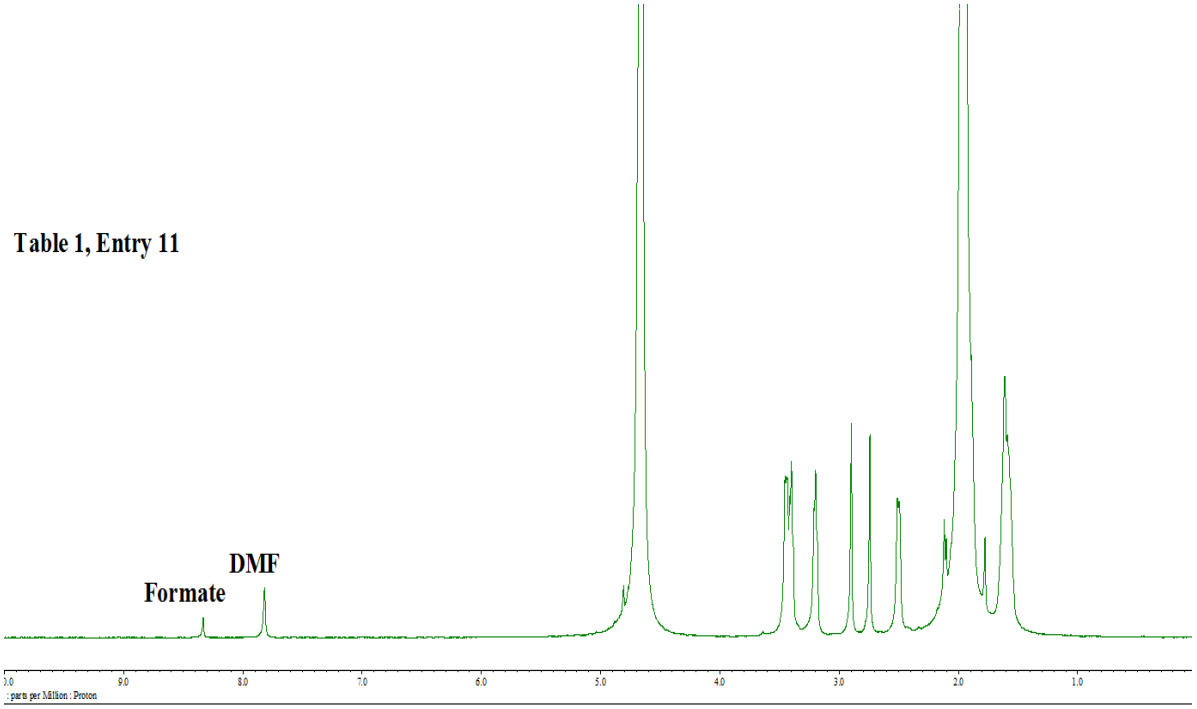

Figure S35. ^{1}H NMR spectrum for the hydrogenation of CO_2 to formate (Table 1, entry 11).

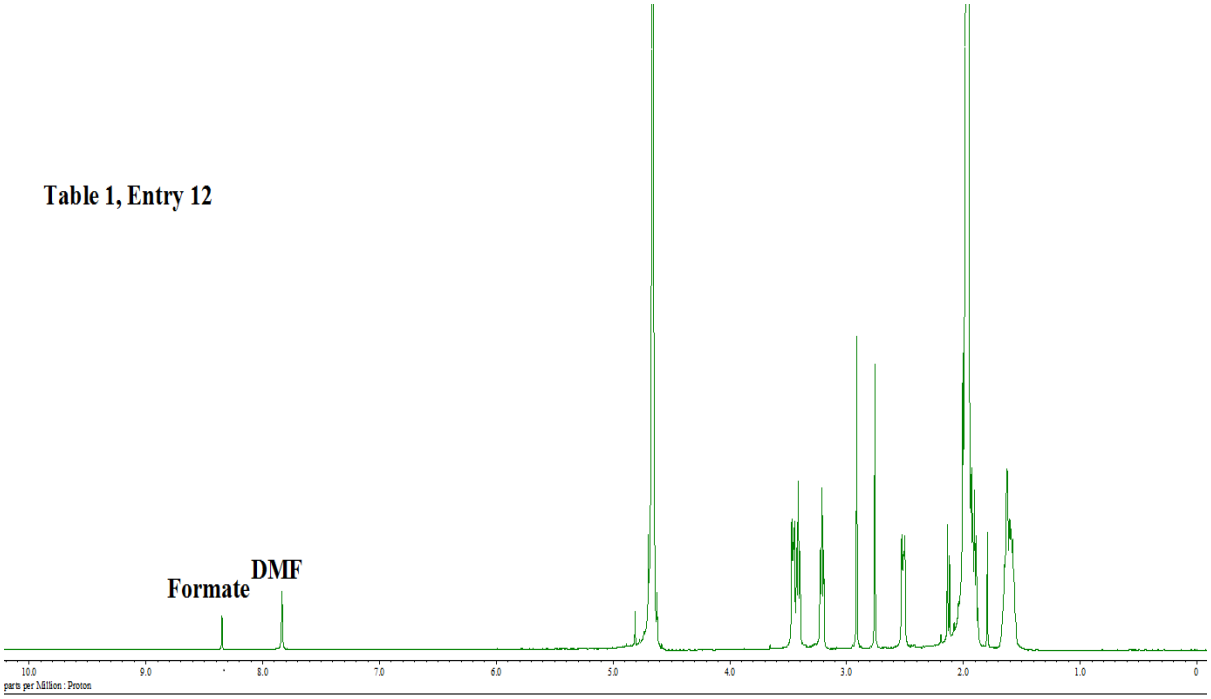

Figure S36. ^{1}H NMR spectrum for the hydrogenation of CO_2 to formate (Table 1, entry 12).

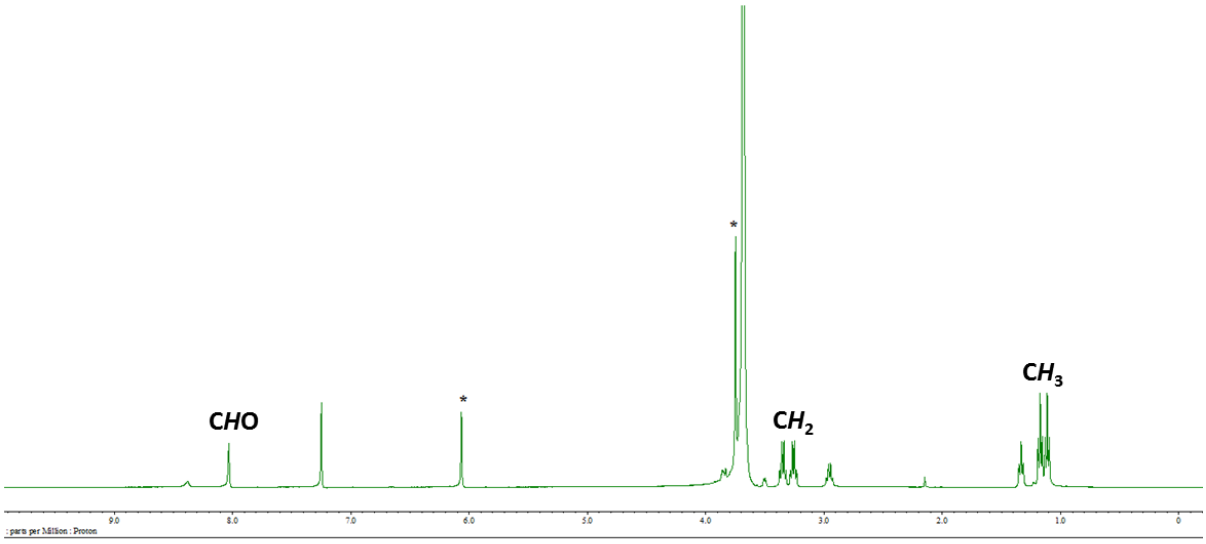

Figure S37. Representative ^{1}H-NMR-spectrum for the hydrogenation of CO_2 to formamide with catalyst **1** in dioxane solvent in the presence of diethylamine (Table S6, entry 2). Peaks marked with an asterisk* belong to the internal standard (1,3,5-trimethoxybenzene).

FT-IR spectra of Mn complexes

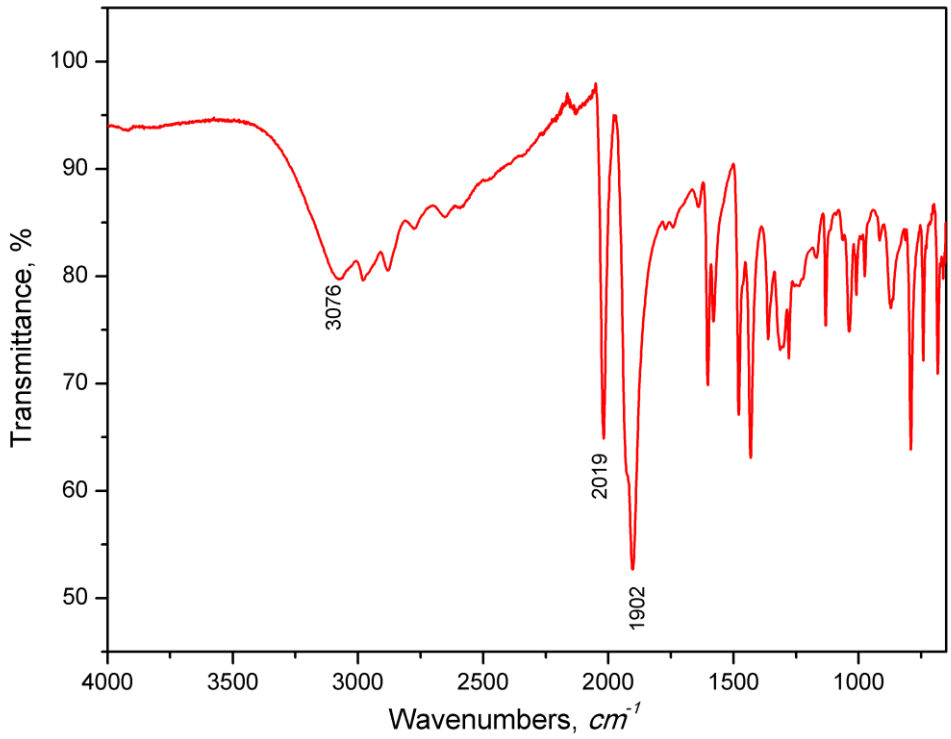

Figure S38. FT-IR (ATR) spectrum of complex **1** (solid).

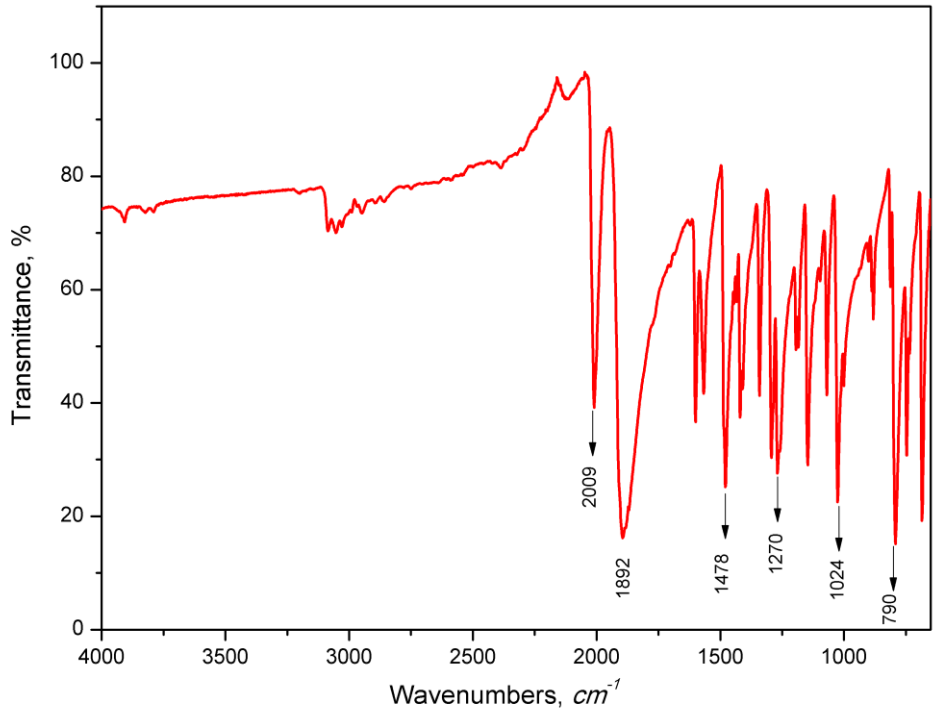

Figure S39. FT-IR (ATR) spectrum of complex **3** (solid).

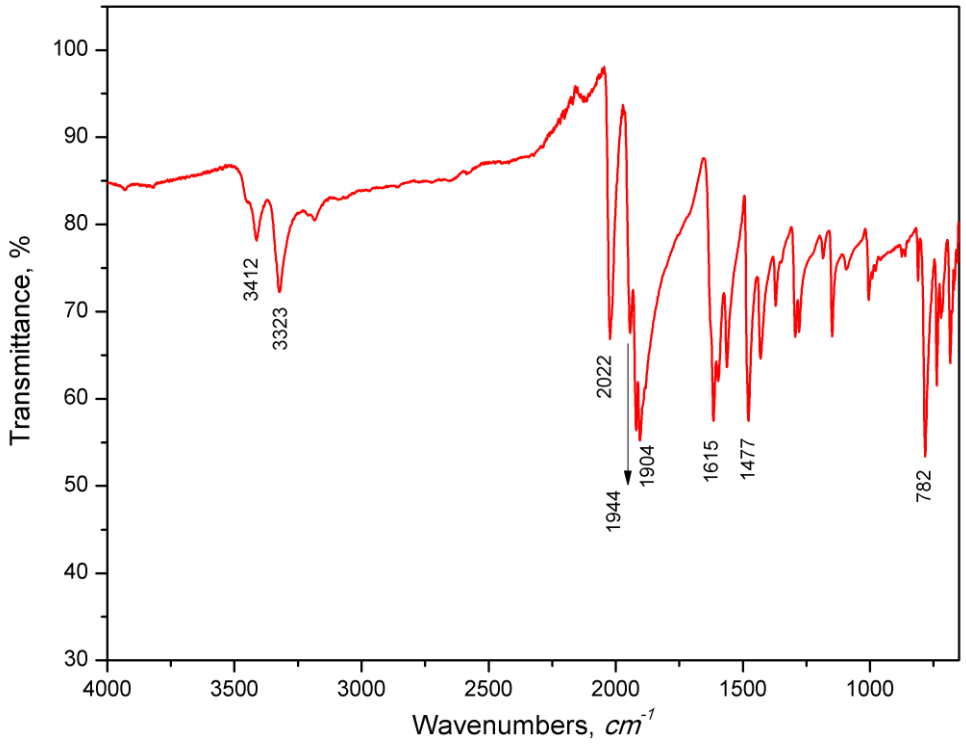

Figure S40. FT-IR (ATR) spectrum of complex **4** (solid).

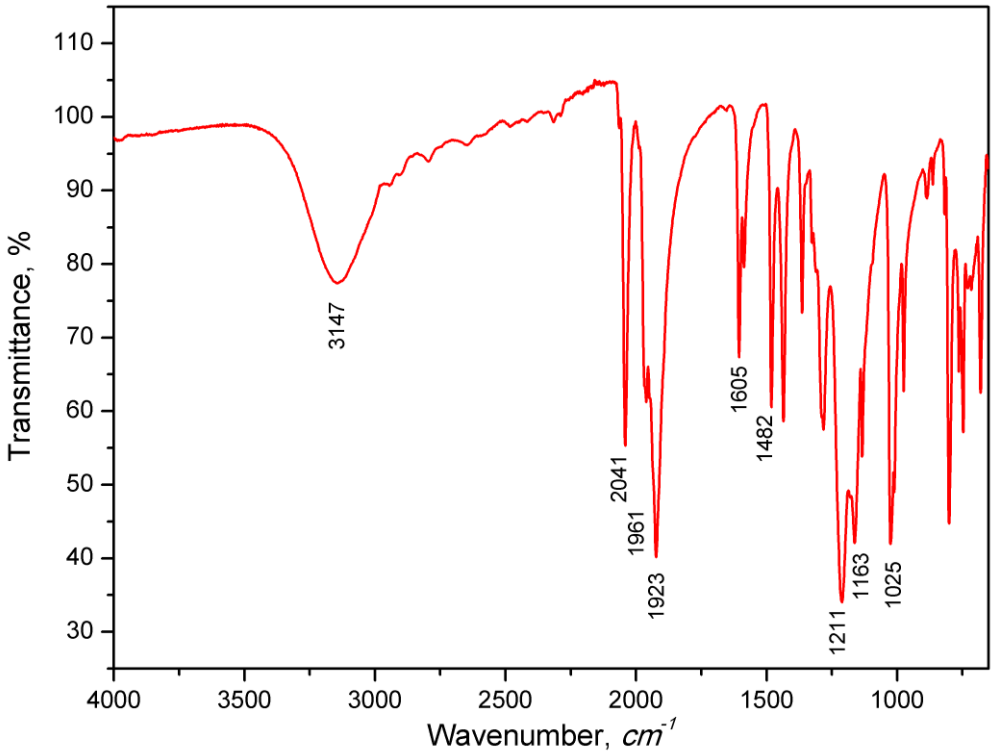

Figure S41. FT-IR (ATR) spectrum of complex **6** (solid).

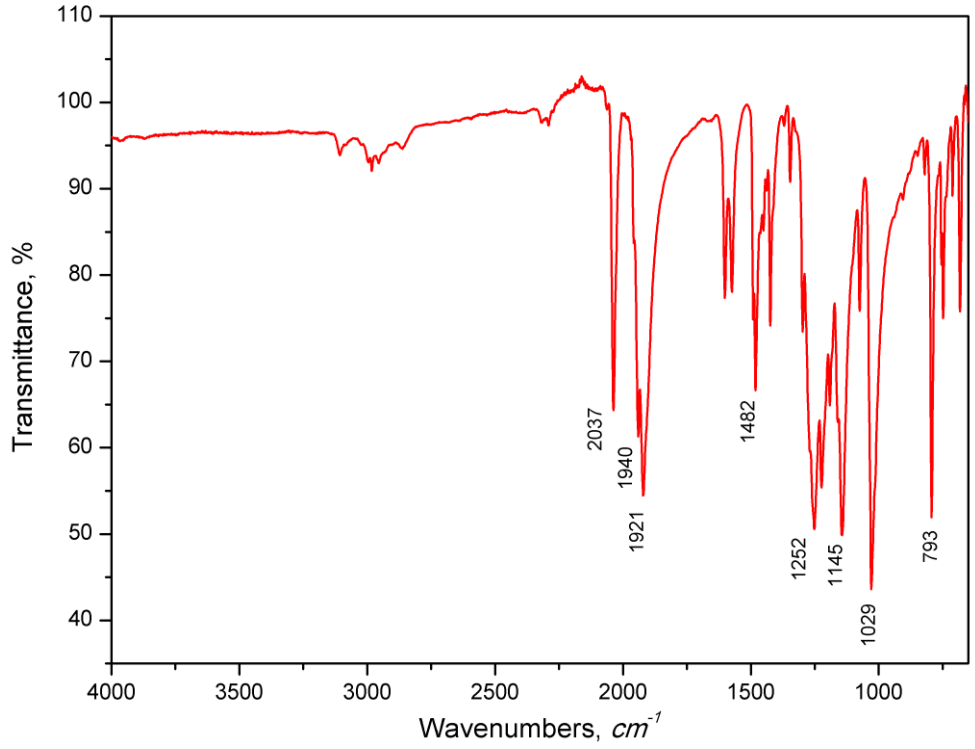

Figure S42. FT-IR (ATR) spectrum of complex **7** (solid).

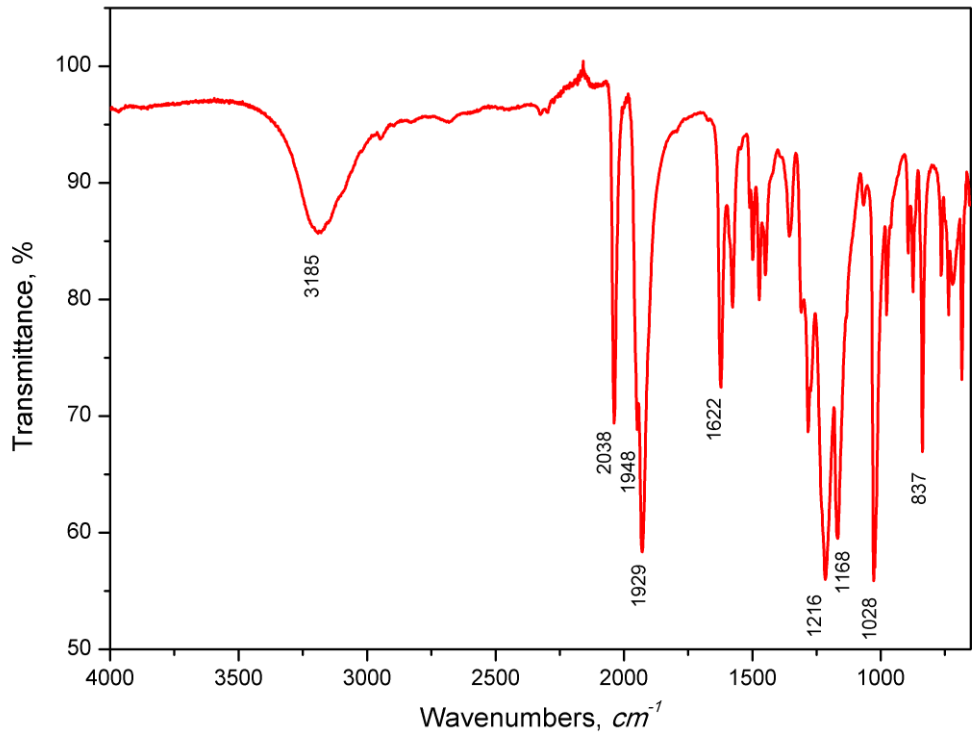

Figure S43. FT-IR (ATR) spectrum of complex **8** (solid).

UV-vis spectra of Mn complexes

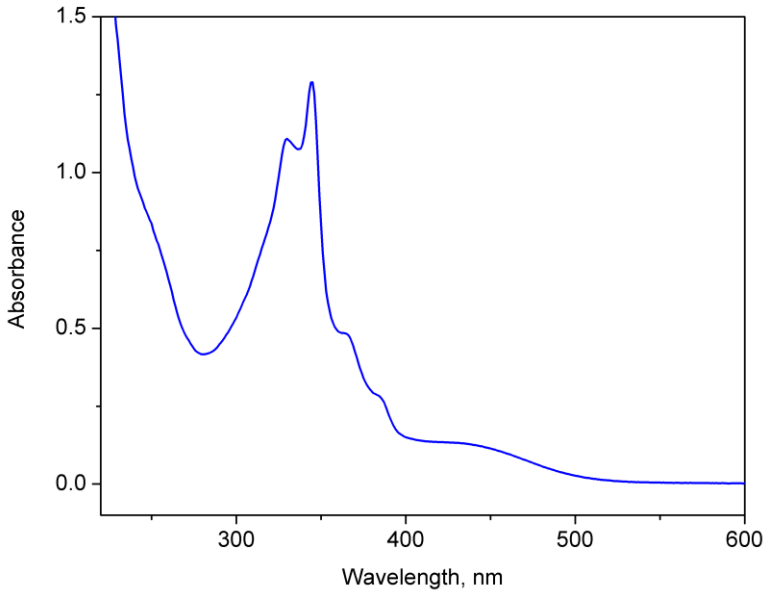

Figure S44. UV-vis spectrum of complex **1** in THF.

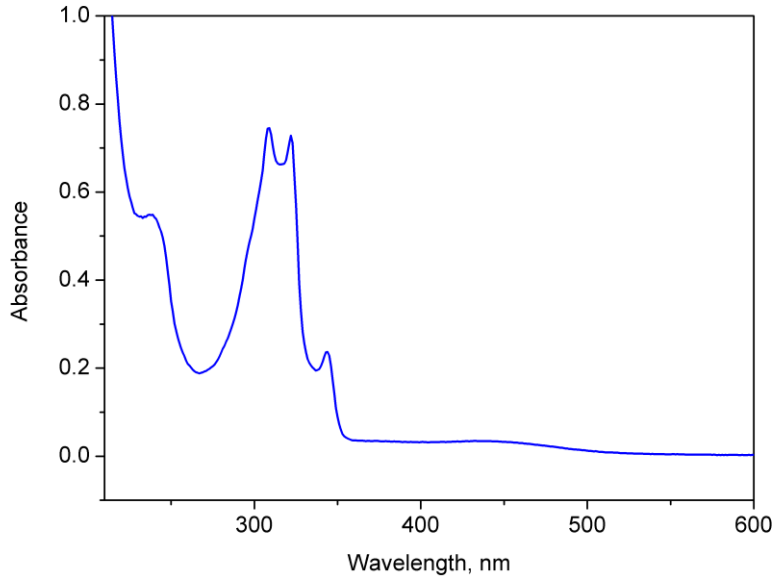

Figure S45. UV-vis spectrum of complex **3** in THF.

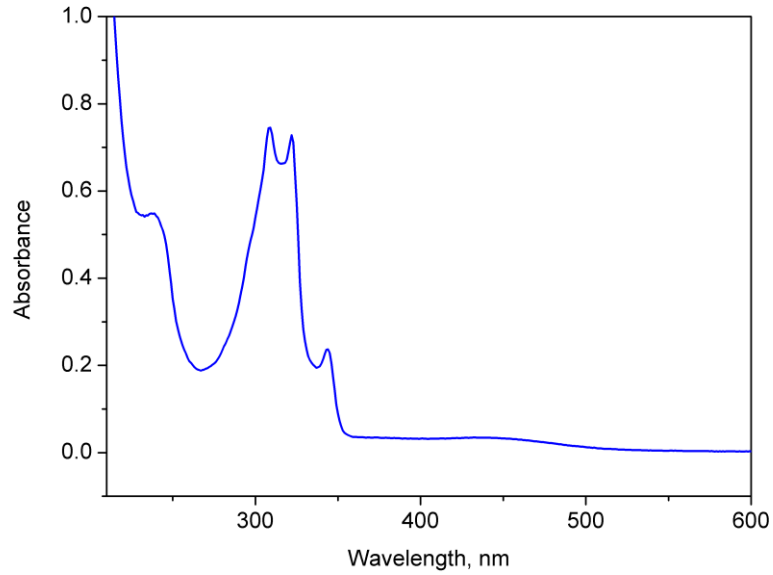

Figure S46. UV-vis spectrum of complex **4** in THF.

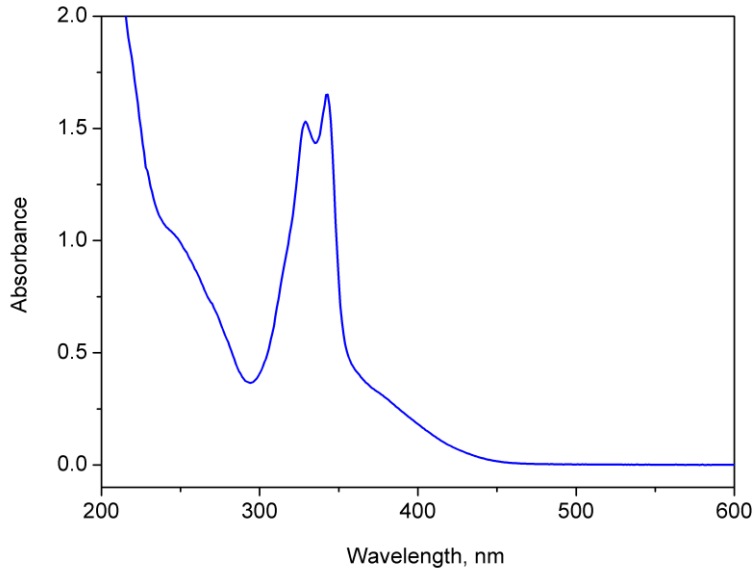

Figure S47. UV-vis spectrum of complex **6** in MeCN.

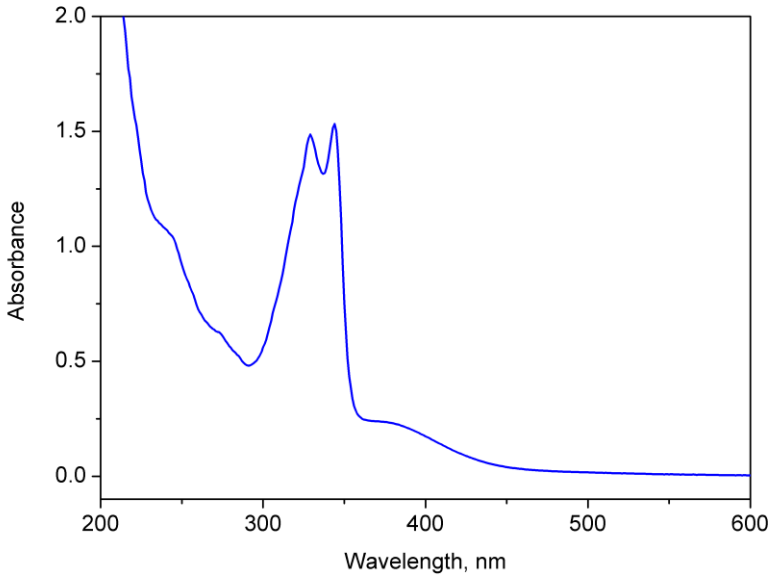

Figure S48. UV-vis spectrum of complex **7** in MeCN.

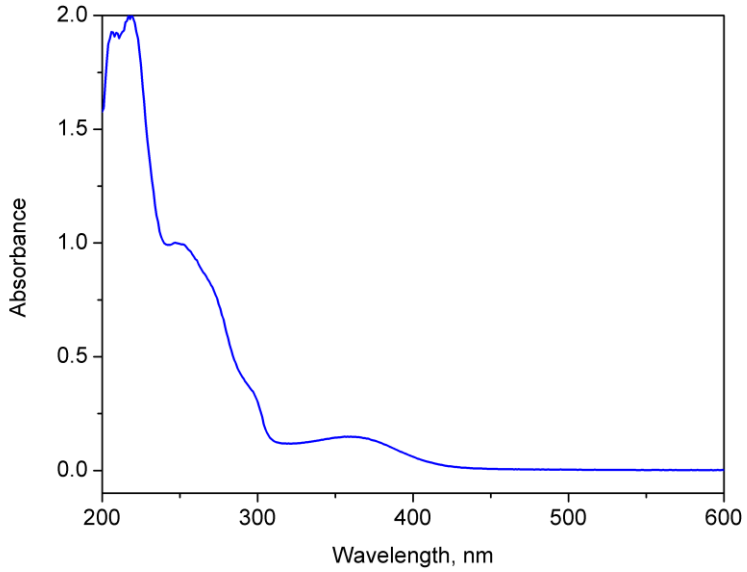

Figure S49. UV-vis spectrum of complex **8** in MeCN.

Trace metal analysis of Pt-group metals by ICP-MS

Sample preparation

Stock solutions containing a commercial standard or synthesized samples were prepared in ultra-pure water that was passed through an element filter (Q-POD Element, Merck Millipore, Billerica, MA, USA). The solutions were ultra-sonicated for 60 minutes at room temperature to achieve the complete dissolution of the standard and samples. A portion of the stock solution was diluted further with an a 5% ultra-pure HNO_3 solution (Ultrapure 100, Kanto Chemical, Tokyo, Japan) to obtain a 0.5 mgL^{-1} solution. In addition, ultrapure water was treated as the same manner as the sample to produce a control 5% HNO_3 solution. This HNO_3 solution was used to determine the blank values for the measurements.

ICP-MS measurement

^{55}Mn, ^{101}Ru, ^{103}Rh, ^{105}Pd, ^{189}Os, ^{193}Ir, and ^{195}Pt were measured using high resolution inductivity coupled plasma high resolution mass spectrometry (ICP-HRMS, ELEMENT 2, Thermo Fisher Scientific, Waltham, MA, USA). The parameters used for the ICP-HRMS measurements are as follows: plasma power 1250 [Watt]; peristatic pump speed 10 [rpm]; cool gas 16 [$Lmin^{-1}$]; aux gas 0.8 [$Lmin^{-1}$]; sample gas 1.06 [$Lmin^{-1}$]; mass window 125 [%]; segment duration 1.25 [s]; sample time 0.05 [s]; sample per peak 20; search window 60 [%]. The mass spectrometer was operated in a high-resolution mode with R = 10000. The mass ranges used for the measurements were *m/z* 54.934 - 54.941 for ^{55}Mn, *m/z* 100.899 - 100.911 for ^{101}Ru, *m/z* 102.899 - 102.911 for ^{103}Rh, *m/z* 104.898 - 104.911 for ^{105}Pd, *m/z* 188.946 - 188.969 for ^{189}Os, *m/z* 192.950 - 192.974 for ^{193}Ir, *m/z* 194.952 - 194.976 for ^{195}Pt. The mass calibration was performed using a multi-element ICP-MS tune-up solution (Thermo Fisher Scientific).

Conclusion

Table S8 summarizes the data obtained from the ICP-HRMS measurements for ultrapure water, 5% HNO_3, commercially available standard, and synthesized samples. No quantifiable levels of Pt group elements or Mn were measured in ultrapure water and the 5% HNO_3 solution. Noticeably elevated levels of Mn were detected in the standard compound and samples owing to their Mn carbonyl structures. In comparison, the signals for Pt group elements were at the levels of the blank solutions, indicating they were not present in the samples.

Table S8. Summary of ICP-HRMS measurements for Pt group elements and Mn. Numbers are given in counts per second (cps).

	Ultrapure water	5% HNO_3	$Mn(CO)_5Br$	Complex **1**	Complex **6**
	cps	cps	cps	cps	cps
^{55}Mn	7.2	3.7	31791	6369	40406
^{101}Ru	1.2	0.1	0.6	0.6	0.3
^{103}Rh	0.6	0.5	0.5	0.3	0.8
^{105}Pd	0.4	0.4	0	0.3	0
^{189}Os	0.3	0.4	0.1	0	0
^{193}Ir	0	0	0	0	0
^{195}Pt	0	0	0	0	0.1

X-ray structure determination details

The crystallographic data for the investigated compounds have been deposited in the Cambridge Crystallographic Data Centre as supplementary publication numbers CCDC 1531371 (**1**), 1531372 (**3**), 1531373 (**4**), 1531374 (**6**), 1531375 (**7**). These data can be obtained free of charge via www.ccdc.cam.ac.uk/data_request/cif, or by emailing data_request@ccdc.cam.ac.uk, or by contacting The Cambridge Crystallographic Data Centre, 12 Union Road, Cambridge CB2 1EZ, UK; fax: +44 1223 336033.

The X-ray diffraction data for the single crystals were collected on a Rigaku XtaLab PRO instrument (ω-scan mode) using graphite monochromated MoKα radiation (0.71073 Å). The diffractometer was equipped with a Rigaku GN2 low temperature system (air cooling type) for low temperature experiments. The performance mode of the microfocus sealed X-ray tube was 50 kV, 0.60 mA. Suitable crystals of appropriate dimensions were mounted on loops in random orientations. Preliminary unit cell parameters were determined with three sets of total 30 narrow frame scans. Data collection: images were indexed and integrated using CrysAlisPro data reduction package (version 1.171.39.7b, Rigaku Oxford Diffraction, 2015). Analysis of the integrated data did not show any decay. Final cell constants were determined by global refinement of reflections from the complete data set. Data were corrected for systematic errors and absorption using the ABSPACK module. The structures were solved by the direct intrinsic phasing method using SHELXT-2014/5[5] and refined by the full matrix least-squares on F^2 using SHELXL-2016/6.[6] Non-hydrogen atoms were refined anisotropically. The position of the hydrogen atoms of hydroxy (for **1** and **6**) and amino (for **4**) groups was determined on the basis of the electronic density distribution, and these atoms were refined isotropically. The other hydrogen atoms were inserted at the calculated positions and refined as riding atoms. The crystal data, data collection and structure refinement details for the five investigated crystals are summarized in Table S9.

Interestingly, complex **1** crystallizes with two molecules A and B bisected by mirror planes, hence the asymmetric cell contains half of both molecules ($Z' = 0.5 + 0.5 = 1$). Two molecules A and B are present in the asymmetric cell ($Z' = 2$) of compound **6**. Complexes **3**, **4**, and **7** crystallize with only the symmetry independent molecule in the unit cell.

All analyzed complexes are characterized by octahedral coordination at the central Mn(I) ion with Br or MeCN ligands present in an axial position relative to the plane of bipyridyl ligand; CO ligands occupy the rest of the positions. Molecular structures of the investigated complexes in the crystalline phase and accepted partial numbering are presented as ORTEP diagrams in Figures S50-S54. Selected bond lengths and angles are appended to the captions.

As illustrated in Figures S55-S56 and suggested in Tables S10-S11, the primary supramolecular motifs in the crystals of **1** and **6** are 1D chains supported by classical

intermolecular hydrogen bonds.

The crystal structure of **1** contains empty solvent-accessible voids of 54 Å^3 (the packing index is 69.1 %). At the same time, the packing of rigid molecules of **1** provides a strong hydrogen bonded supramolecular system. (Figure S55 and Table S7) The absence of residual electron density in the voids was verified on a difference Fourier map and with PLATON's SQUEEZE function.[7]

Table S9. Crystallographic data summary for the investigated complexes.

Compound	**1**	**3**	**4**	**6**	**7**
File name	jk092	jk124	jk147	jk070	jk130
CCDC number	1531371	1531372	1531373	1531374	1531375
Formula	$C_{13}H_8BrMnN_2O_5$	$C_{15}H_{12}BrMnN_2O_5$	$C_{13}H_{10}BrMnN_4O_3$	$C_{16}H_{11}F_3MnN_3O_8S$	$C_{18}H_{15}F_3MnN_3O_8S$
Colour	yellow	yellow	yellow	yellow	yellow
Formula weight	407.06	435.12	405.10	517.28	545.33
Temperature, K	100(2)	93(2)	110(2)	93(2)	105(2)
Crystal system	orthorhombic	monoclinic	monoclinic	triclinic	monoclinic
Space group	*Pbam*	$P2_1/n$	$P2_1/n$	$P\bar{1}$	$P2_1/c$
Cell parameters: *a*, *b*, *c* (Å) and α, ß, γ (deg)	17.7576(10), 12.9229(7), 12.7518(7) and 90, 90, 90	8.1795(5), 16.3907(11), 11.9305(6) and 90, 90.478(5), 90	7.5829(2), 9.6475(3), 20.0238(5) and 90, 93.812(3), 90	8.91210(19), 12.7125(3), 17.6682(4) and 84.4838(18), 86.3815(18), 83.4002(17)	8.19264(16), 11.4621(3), 23.0399(5) and 90, 92.2861(19), 90
Volume, Å^3	2926.3(3)	1599.44(16)	1461.62(7)	1976.50(7)	2161.82(8)
Z and *Z*′	8 and 1 (0.5 + 0.5)	4 and 1	4 and 1	4 and 2	4 and 1
Calculated density, g cm^{-3}	1.848	1.807	1.841	1.738	1.676
Absorption coefficient, mm^{-1}	3.657	3.352	3.654	0.853	0.785
F(000)	1600	864	800	1040	1104
Crystal size, mm^3	0.069 x 0.151 x 0.221	0.016 x 0.046 x 0.155	0.038 x 0.100 x 0.158	0.100 x 0.114 x 0.250	0.149 x 0.198 x 0.266

Table S9 (continues). Crystallographic data summary for the investigated complexes.

Compound	**1**	**3**	**4**	**6**	**7**
Θ range, deg	3.195 to 28.899	2.485 to 28.497	2.344 to 30.700	2.633 to 27.895	2.995 to 29.998
Index ranges	-24 ≤ *h* ≤ 18, -17 ≤ *k* ≤ 16, -16 ≤ *l* ≤ 17	-10 ≤ *h* ≤ 10, -21 ≤ *k* ≤ 21, -16 ≤ *l* ≤ 15	-10 ≤ *h* ≤ 10, -13 ≤ *k* ≤ 13, -28 ≤ *l* ≤ 28	-11 ≤ *h* ≤ 11, -16 ≤ *k* ≤ 16, -23 ≤ *l* ≤ 21	-11 ≤ *h* ≤ 11, -16 ≤ *k* ≤ 15, -31 ≤ *l* ≤ 32
Measured and independent reflections [*R*(int)]	18071 and 4011 [0.0611]	32877 and 4012 [0.0684]	39579 and 4505 [0.0480]	25832 and 8797 [0.0329]	39259 and 6276 [0.0257]
Observed Data [*I* > 2σ(*I*)]	3156	3562	4061	7811	5838
Completeness to Θ = 25.242°, %	99.7	99.9	99.8	99.6	99.8
Data, restraints, parameters	4011, 0, 219	4012, 0, 219	4505, 0, 215	8797, 0, 595	6276, 0, 310
Goodness-of-fit on F^2	1.017	1.033	1.044	1.061	1.052
*R*1 and *wR*2 indices [*I* > 2σ(*I*)]	0.0356 and 0.0800	0.0310 and 0.0727	0.0241 and 0.0571	0.0286 and 0.0717	0.0253 and 0.0667
*R*1 and *wR*2 indices (all data)	0.0535 and 0.0852	0.0382 and 0.0753	0.0291 and 0.0585	0.0332 and 0.0738	0.0277 and 0.0678
Largest diff. hole and peak, e Å^{-3}	-0.920 and 0.588	-0.388 and 0.824	-0.282 and 1.519	-0.496 and 0.420	-0.378 and 0.433

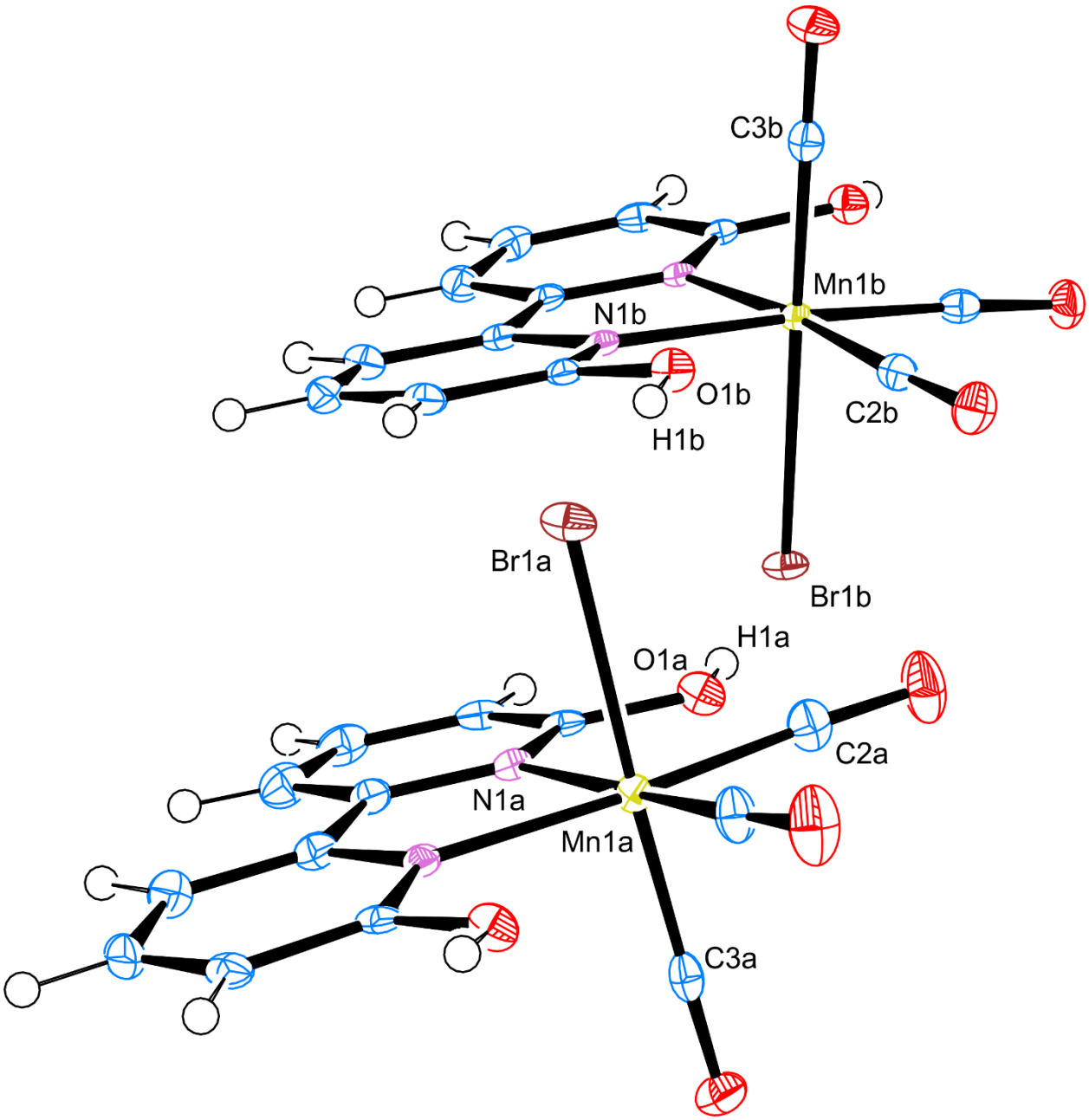

Figure S50. ORTEP diagram showing 50 % probability anisotropic displacement ellipsoids of non-hydrogen atoms for complex **1** in crystals. Selected bond lengths and angles (Å, °): Mn1A–N1A 2.0817(19), Mn1A–Br1A 2.5823(6), Mn1A–C2A 1.819(2), Mn1A–C3A 1.790(4), Br1A–Mn1A–N1A 88.94(5), Br1A–Mn1A–C2A 88.34(8), Br1A–Mn1A–C3A 177.66(11), Mn1B–N1B 2.0622(19), Mn1B–Br1B 2.5722(6), Mn1B–C2B 1.812(2), Mn1B–C3B 1.784(4), Br1B–Mn1B–N1B 87.30(5), Br1B–Mn1B–C2B 88.11(8), Br1B–Mn1B–C3B 179.40(11).

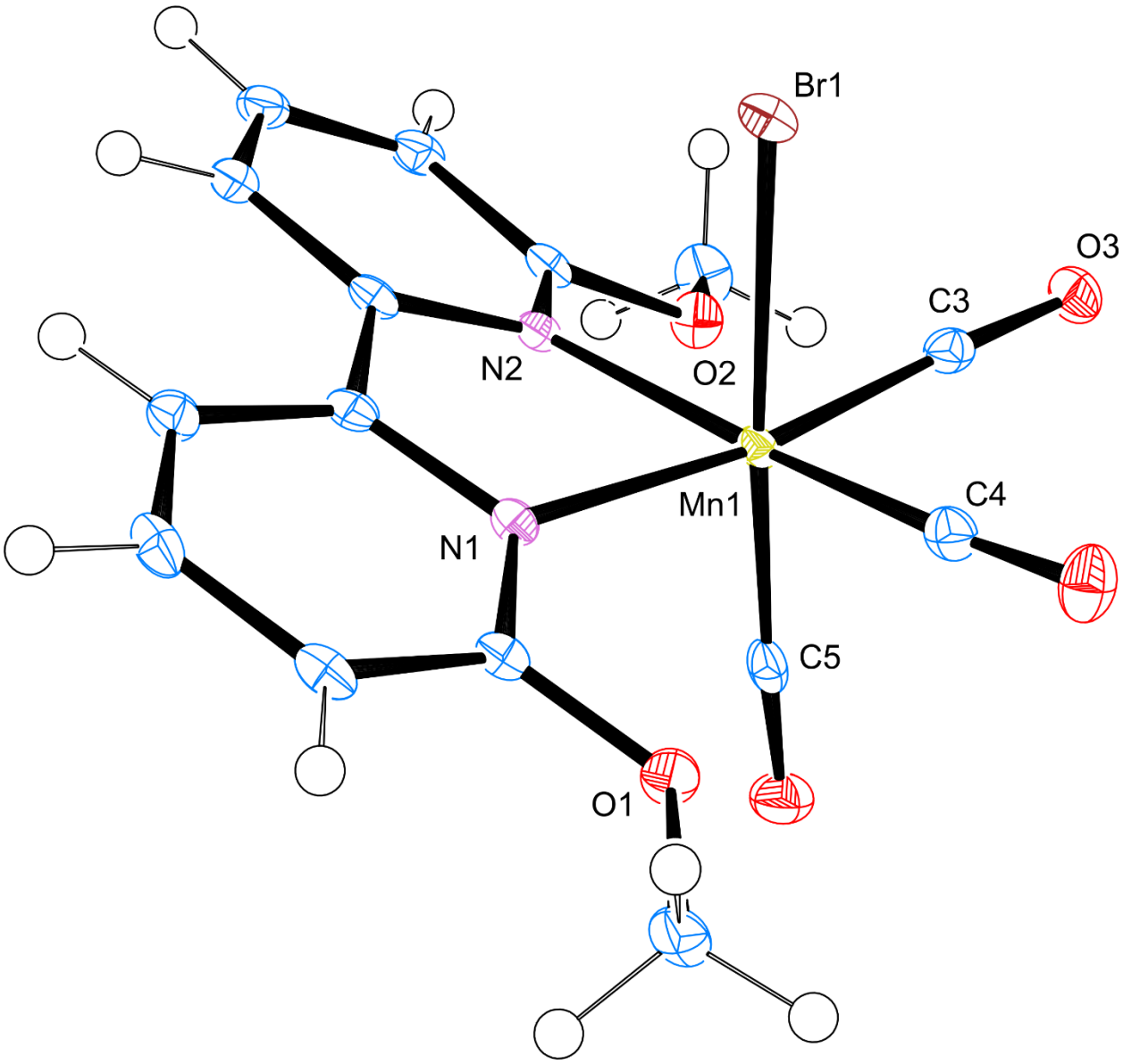

Figure S51. ORTEP diagram showing 50 % probability anisotropic displacement ellipsoids of non-hydrogen atoms for complex **3** in crystals. Selected bond lengths and angles (Å, °): Mn1–N1 2.0609(17), Mn1–N2 2.0586(17), Mn1–Br1 2.5373(4), Mn1–C3 1.807(2), Mn1–C4 1.807(2), Mn1–C5 1.803(2), Br1–Mn1–N1 86.82(5), Br1–Mn1–N2 86.35(5), Br1–Mn1–C3 85.90(7), Br1–Mn1–C4 86.59(7), Br1–Mn1–C5 176.29(7).

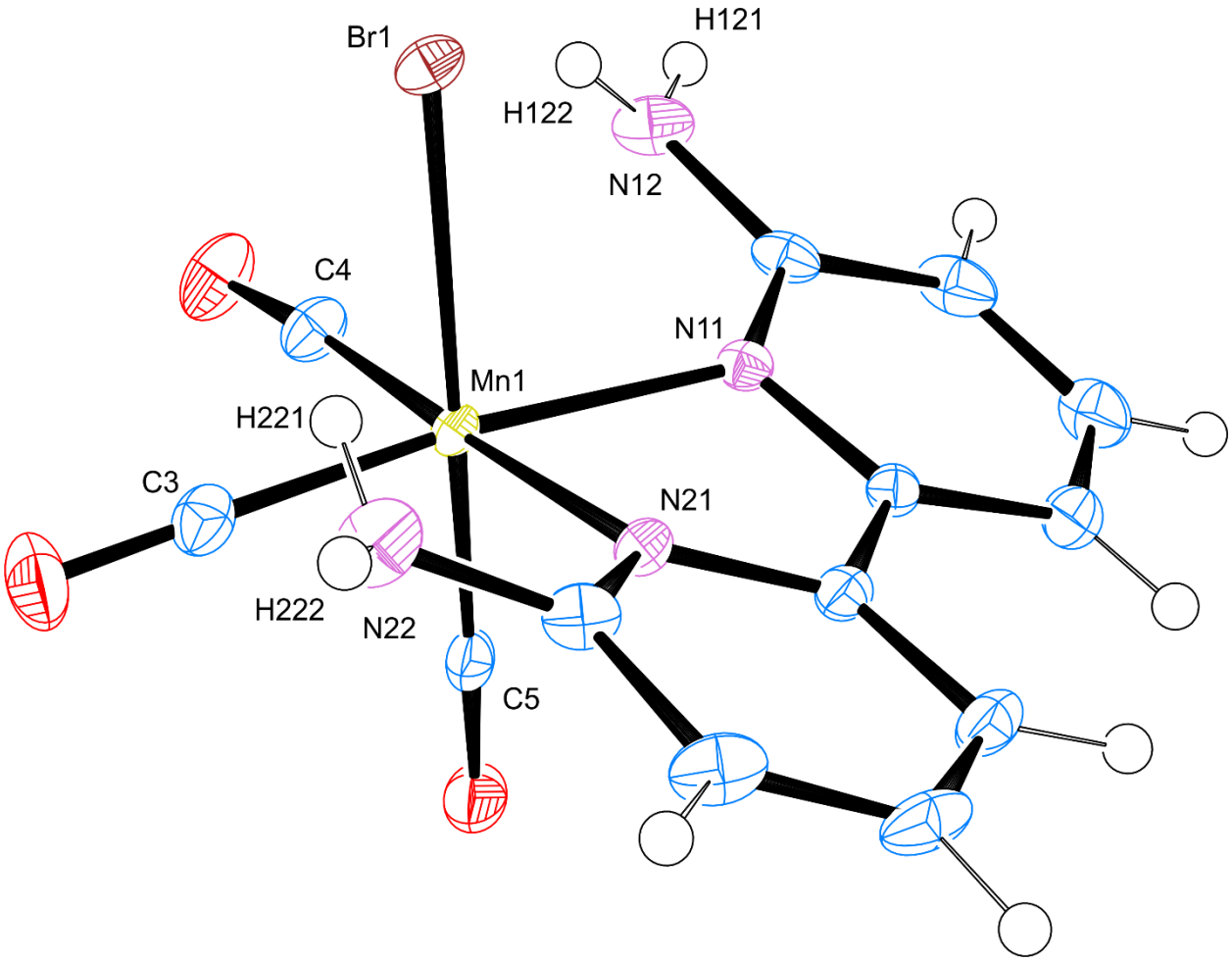

Figure S52. ORTEP diagram showing 50 % probability anisotropic displacement ellipsoids of non-hydrogen atoms for complex **4** in crystals. Selected bond lengths and angles (Å, °): Mn1–N11 2.0785(13), Mn1–N21 2.0672(12), Mn1–Br1 2.5771(3), Mn1–C3 1.8166(17), Mn1–C4 1.8157(16), Mn1–C5 1.7906(16), Br1–Mn1–N11 90.98(3), Br1–Mn1–N21 90.55(4), Br1–Mn1–C3 94.01(5), Br1–Mn1–C4 88.69(5), Br1–Mn1–C5 176.25(5).

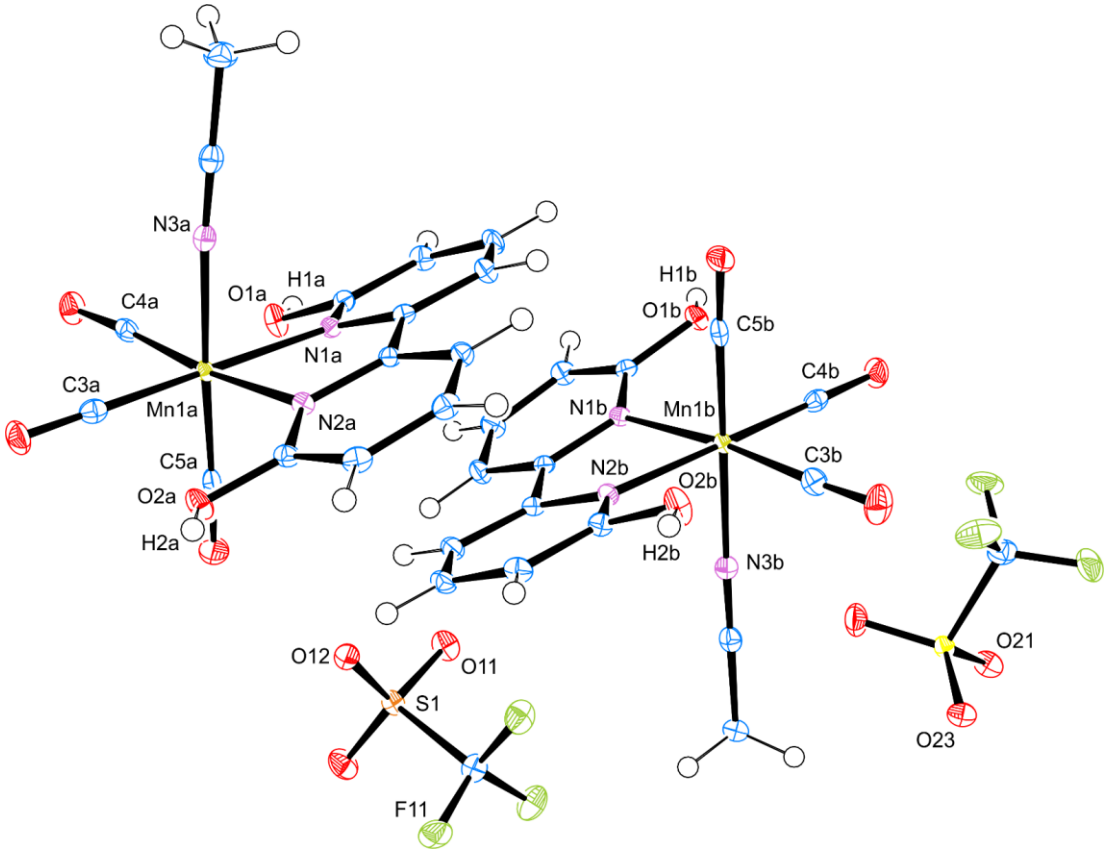

Figure S53. ORTEP diagram showing 50 % probability anisotropic displacement ellipsoids of non-hydrogen atoms for complex **6** in crystals. Selected bond lengths and angles (Å, °): Mn1A–N1A 2.0772(13), Mn1A–N2A 2.0734(13), Mn1A–N3A 2.0360(13), Mn1A–C3A 1.8369(17), Mn1A–C4A 1.8150(16), Mn1A–C5A 1.8074(16), N3A–Mn1A–N1A 83.97(5), N3A–Mn1A–N2A 83.32(5), N3A–Mn1A–C3A 94.57(6), N3A–Mn1A–C4A 90.37(6), N3A–Mn1A–C5A 176.24(6), Mn1B–N1B 2.0779(13), Mn1B–N2B 2.0734(13), Mn1B–N3B 2.0365(13), Mn1B–C3B 1.8186(16), Mn1B–C4B 1.8359(16), Mn1B–C5B 1.8020(16), N3B–Mn1B–N1B 85.81(5), N3B–Mn1B–N2B 84.49(5), N3B–Mn1B–C3B 88.67(6), N3B–Mn1B–C4B 93.34(6), N3B–Mn1B–C5B 177.46(6).

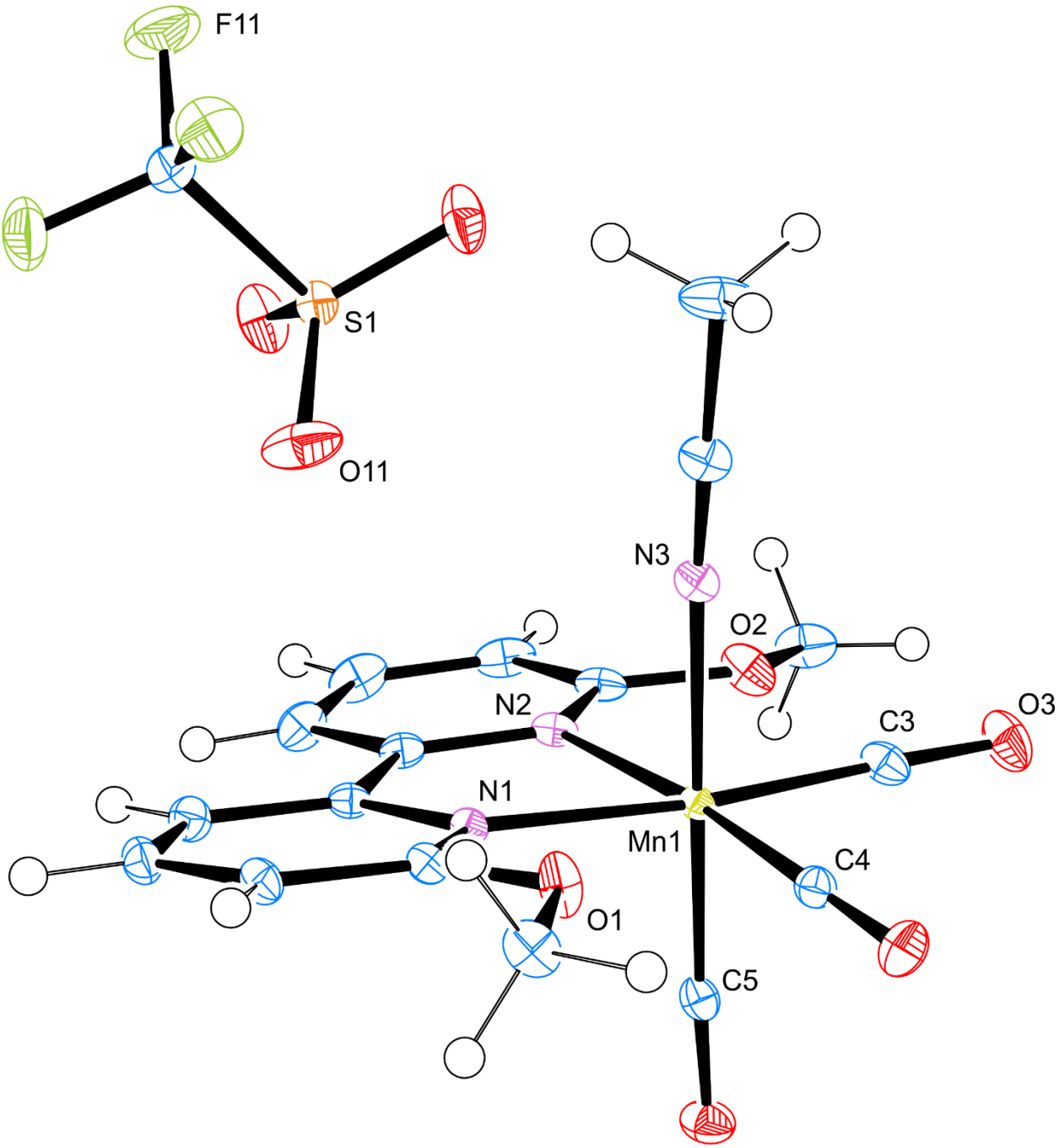

Figure S54. ORTEP diagram showing 50 % probability anisotropic displacement ellipsoids of non-hydrogen atoms for complex **7** in crystals. Selected bond lengths and angles (Å, °): Mn1–N1 2.0848(9), Mn1–N2 2.1041(9), Mn1–N3 2.0266(9), Mn1–C3 1.8194(11), Mn1–C4 1.8165(11), Mn1–C5 1.8157(11), N3–Mn1–N1 84.98(4), N3–Mn1–N2 91.76(4), N3–Mn1–C3 90.19(4), N3–Mn1–C4 91.42(4), N3–Mn1–C5 177.89(4).

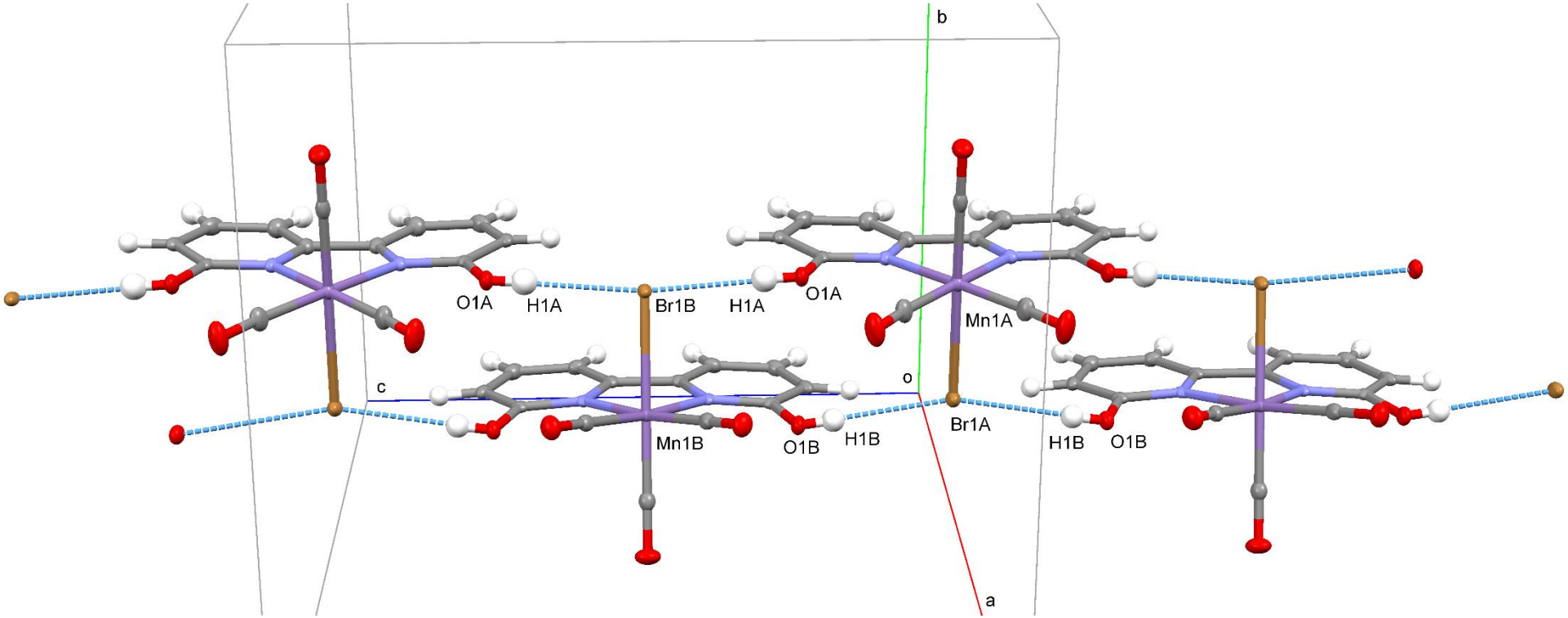

Figure S55. A fragment of the molecular packing in the crystals of **1**: perspective projection. Hydrogen bonds are marked in dotted blue lines. Thermal ellipsoids for non-hydrogen atoms and spheres for hydrogen atoms are shown at 50% probability level.

Table S10. Parameters of the intermolecular hydrogen bonds for complex **1** in the crystals.

D–H···A	d(D–H), Å	d(H···A), Å	d(D···A), Å	∠ DHA, °
O1A–H1A···Br1B	0.77(3)	2.46(3)	3.2244(17)	178(3)
O1B–H1B···Br1A	0.73(3)	2.53(3)	3.2629(17)	178(3)

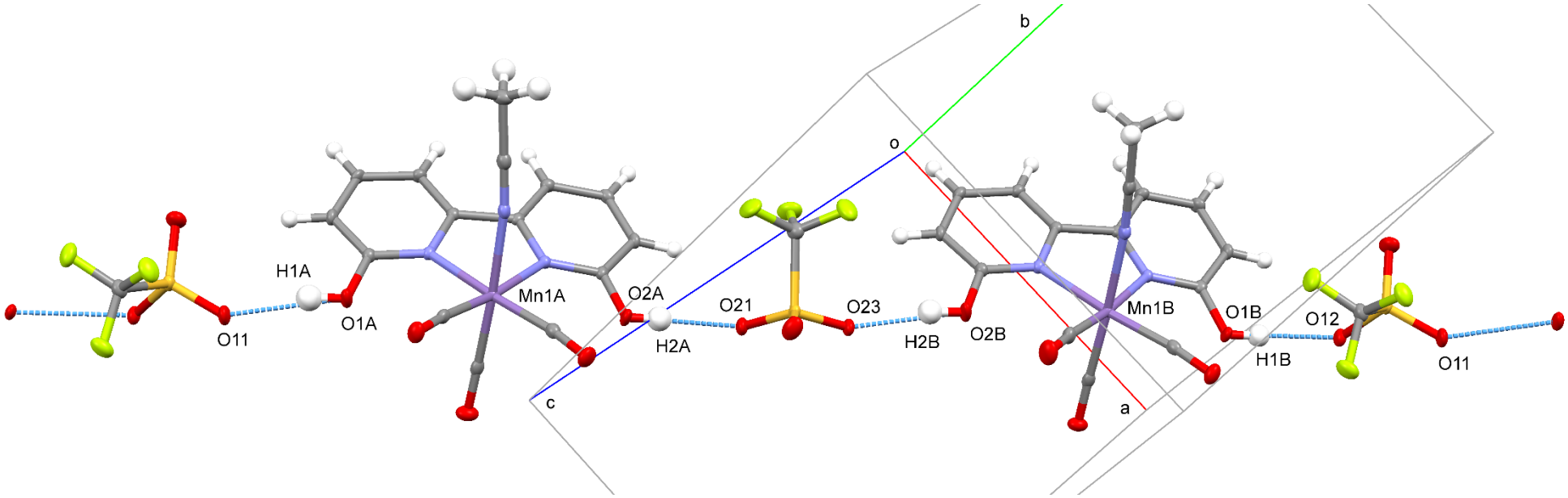

Figure S56. A fragment of the molecular packing in the crystals of **6**: perspective projection. Hydrogen bonds are marked in dotted blue lines. Thermal ellipsoids for non-hydrogen atoms and spheres for hydrogen atoms are shown at 50% probability level.

Table S11. Parameters of the intermolecular hydrogen bonds for complex **6** in the crystals.

D–H···A	d(D–H), Å	d(H···A), Å	d(D···A), Å	∠ DHA, °	Symmetry operation
O1A–H1A···O11	0.82(2)	1.91(3)	2.7153(16)	167(2)	–x + 1, –y + 1, –z + 2
O2A–H2A···O21	0.77(2)	1.94(2)	2.7069(16)	177(3)	x + 1, y + 1, z
O1B–H1B···O12	0.79(2)	1.92(2)	2.7084(15)	172(2)	x – 1, y, z
O2B–H2B···O23	0.81(2)	1.88(2)	2.6769(16)	168(2)	–x + 1, –y + 1, –z + 1

References:

(1) Bourrez, M.; Molton, F.; Chardon-Noblat, S.; Deronzier, A. *Angew. Chem., Int. Ed.* **2011**, *50*, 9903-9906.

(2) Walsh, J. J.; Smith, C. L.; Neri, G.; Whitehead, G. F. S.; Robertson, C. M.; Cowan, A. J. *Faraday Discuss.* **2015**, *183*, 147-160.

(3) Cocco, F.; Cinellu, M. A.; Minghetti, G.; Zucca, A.; Stoccoro, S.; Maiore, L.; Manassero, M. *Organometallics* **2010**, *29*, 1064-1066.

(4) Hong, Y.-R.; Gorman, C. B. *J. Org. Chem.* **2003**, *68*, 9019-9025.

(5) Sheldrick, G. M. *Acta Crystallogr., Sect. A: Found. Adv.* **2015**, *71*, 3-8.

(6) Sheldrick, G. M. *Acta Crystallogr., Sect. C: Struct. Chem.* **2015**, *71*, 3-8.

(7) Spek, A. L. *Acta Crystallogr., Sect. C: Struct. Chem.* **2015**, *71*, 9-18.